ABSTRACT

New technology has increased the potential digital information carrying capacity of copper twisted pairs currently used for telephone service. The ability to deliver video channels over existing twisted pairs depends on the limitations of the loop plant. At high data rates, a major limitation on bandwidth is the attenuation of the transmission line. The capability to characterize these lines becomes essential. Similarly on the board packaging level, the performance of integrated circuits is limited by interconnects. When interconnects are sufficiently long relative to a wavelength, the interconnects must be modeled as transmission lines. This project involves the characterization of transmission lines (be they coaxial, twisted pair, or microstrip) using scattering parameter measurements made using a network analyzer over the bandwidth of interest. A simple approximation allows for the extraction of the line characteristics.

ACKNOWLEDGMENTS

I would like to thank my advisor, Professor Jose Schutt-Aine for his support and his selection of this thesis topic. I would also like to thank Professor Paul Klock for being an invaluable resource; Karen Coperich who was always eager to help; and my parents, for their continued support in my endeavors.

TABLE OF CONTENTS

CHAPTER 1

INTRODUCTION

1.1 Overview

As advances in digital technologies continue to grow, transmission line characterization becomes increasingly important. New technology has increased the potential digital information carrying capacity of copper twisted pairs currently used for telephone service. The ability to deliver video channels over existing twisted pairs depends on the limitations of the loop plant.

Paralleling the advances made in the communications industry, the demand for smaller integrated circuits and faster digital circuits continue to grow. Modeling of interconnects becomes critical. Interconnects play an increasingly important role in determining the speed, area, and performance of high-speed digital circuits. Microstrip transmission lines are often used in constructing integrated circuit board interconnects.

1.2 The Problem Being Addressed

At high data rates, a major limitation on signal integrity is attenuation and delay distortion for both telephone cables and microstrip interconnects. This work describes the development of a measurement technique that may be applied toward characterizing transmission lines, whether they be microstrip, coaxial, or twisted pair.

1.3 Organization of This Thesis

This thesis will develop a measurement technique that will allow for the extraction of transmission line characteristics and L, R, G, and C parameters over a frequency range spanning multiple wavelengths. Chapter 2 will introduce the telephony and packaging interconnect environments, thus providing the motivation for transmission line characterization. Chapter 3 provides basic transmission line theory and background. In Chapter 4, the measurement technique to extract the sought-after parameters is developed. Chapter 5 contains the summary and conclusion.

CHAPTER 2

BACKGROUND

2.1 Telecommunications

A subscriber line is the basic access connection of a telephone user to the telephone network. It is the means by which the customer transmits information to a local switch to be distributed to other customers or subscribers of the same network. Consequently, the subscriber line must be relatively inexpensive if network access is to be widespread. For this reason, telephone subscriber lines have been voice frequency analog links until very recently. The principle reason for the analog nature of access was its low cost and bandwidth.

With the advent of inexpensive computers, the demand for data transmission grew. Economics led to the choice of voice frequency modems to provide data transmission at low rates of 300 and 1200 b/s that were initially required by most users. Transmission rate for these modems was still in the voice frequency range. The 1960s and 1970s led to the increase of speeds up to 2.4 kb/s. Sophisticated signal processing and echo cancellation brought this to 4.8 kb/s in the early 1980's. More recently, trellis coded modulation (TCMod) has been used to increase data speed to 4.4 kb/s and combined equalization and coding has produced a 9.2 kb/s rate. All of these techniques use the voice band to transmit data [1].

New technology has increased the potential digital-information-carrying capacity of copper pairs, originally placed to provide plain old telephone service (POTS), to the point where certain leading-edge broadband services can be provided to customers

well in advance of direct fiber access. Recent research indicates that it will be feasible to transmit 1.5 Mb/s or more over the majority of existing nonloaded copper loops [2].

Although the telephone voice channel has a limited bandwidth of 3 kHz, the twisted pair telephone subscriber loop connecting subscriber to central office has a much wider bandwidth, limited only by loop attenuation and the noise environment. The digital subscriber line (DSL), used for integrated services digital network (ISDN) basic rate access channel, has a transmission bandwidth of 40 kHz. The high-bit-rate digital subscriber line (HDSL) developed mainly for repeaterless (T1) service has a transmit signal spectrum of 300 kHz [3]. The asymmetric digital subscriber line (ADSL) will support 1.536 Mb/s on standard twisted-pair telephone lines, unidirectional, from the central office to the customer premises. Discrete multitone (DMT) ADSL has a transmit signal bandwidth of 1.1 MHz. Full duplex POTS service is located below 10 kHz, and the upstream from subscriber to central office digital telephone channels are between 10 kHz and 100 kHz [4].

Initially networks evolved separately from the main public switched telephone network (PSTN); however, it was widely recognized that it would be more economic for PTO (public telecommunication operation) to develop a single network supporting all classes of services. This led to the vision of ISDN, a single digital network which would be capable of supporting both voice and data services [5].

The ISDN basic access system was the first embodiment of DSLs. ISDN uses adaptive digital signal processing for both pulse restoration and cancellation of transmit/receive echoes. It provides 44 kb/s transport in both directions over up to 18 kft of the existing unloaded wire plant. The planned deployment of ISDN was a major motivation for developing video compression techniques.

With high-speed digital signal processing and very large scale integrated (VLSI)

circuit technology, HDSL technology has evolved with the capability to transmit high speed digital data through the existing copper loop plant. Quadrature amplitude modulation (QAM) (16 and 64 point) schemes over 20-220 kHz and 20-154 kHz frequency ranges, respectively, are used to implement HDSL. The HDSL modulation scheme uses two pairs to provide 1.544 Mb/s transport to cover the full carrier serving area (CSA) range. Echo cancellation allows each pair to carry 784 kb/s with full duplex transmission.

HDSL provides capability equivalent to TI technology using existing wire pairs and no special engineering. TI carrier systems have been used in the interoffice plant for many years for high-speed transmission. In TI systems, transmission is disrupted with repeater spacing. Implementation of HDSL will lead to cost saving due to the avoidance of TI repeaters. HDSL and DSL service environment is almost exclusively made up of business customers who are expected to be within 12 kft of a remote terminal, within the range HDSL is restricted.

Asymmetric digital subscriber line (ADSL) technology was proposed to provide repeaterless unidirectional 1.544 Mb/s transport capability along with standard bidirectional POTS and or ISDN basic access channel. A low-rate digital control channel will also be available in the reverse direction over the same single nonloaded twisted copper pair.

Figure 2.1 shows the spectrum allocation for ADSL using QAM pass-band transmission. The transmission rate can be approximately 1.6 Mb/s, forming a high-rate channel from the network to the customer. In this configuration, the transmission bands from 50 to 500 kHz are being considered for the high-rate channel. A low-rate return channel from the customer to the network to provide signaling and control information is expected to occupy a portion of the frequency band below the high-rate channel. This architecture results in three separate signal components appearing

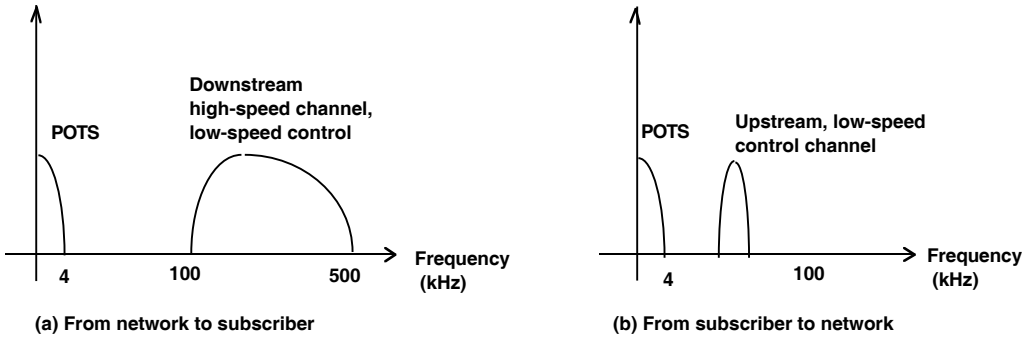

Figure 2.1: An example of spectrum allocation.

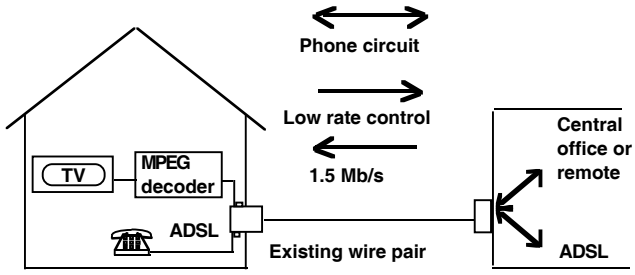

Figure 2.2: A network architecture for a video communication service using an ADSL system.

simultaneously on one wire pair

There are several reasons why ADSL is advantageous in a residential setting. ADSL can operate over one loop pair, while HDSL requires two. ADSL can potentially cover an entire nonloaded loop plant. HDSL is restricted to the CSA range. NEXT (near end crosstalk) does not exist for ADSL. The primary limitations for ADSL are signal loss, crosstalk from other services in binder group, RF interference, and impulse noise.

Figure 2.2 shows a network architecture of potential interfaces for the ADSL system. At the subscriber side, the incoming signal will be demultiplexed into POTS, high-bit-rate signal, and low-bit rate control channel. The POTS line is connected

to an ordinary telephone. The high-bit-rate signal and the low-bit-rate control channel are terminated in a service module. Depending on the applications, this service module can be a Moving Picture Experts Group (MPEG) decoder, a multimedia workstation, or just a personal computer. At the central office, an ADSL system will perform the functions of demultiplexing the upstream POTS signal and control channel, and multiplexing the POTS with the high-bit-rate signal in the downstream direction. Using this architecture, many residential applications such as video-on-demand, interactive multimedia communication, distance learning, and other video services can be offered by the local exchange carriers at an affordable cost in the near future.

As systems like HDSL and ADSL are optimized to squeeze the maximum bandwidth possible out of copper loops, while maintaining predictable and reliable levels of transmission performance, it becomes increasingly important to have an in-depth understanding of loop plant noise sources and topologies. Telephone companies cannot afford to find out if a customer's copper telephone line will support the new digital transmission after installation. They need to keep the number of failed installations to a manageable percentage. If local exchange carriers are to include ADSL or HDSL as one element of their video upgrade strategy, they need to understand precisely what conditions the new technologies require [2].

2.2 Interconnections and Packaging for VLSI

Since the beginning of integrated circuits, the number of devices per chip has been increased by reducing the minimum feature size and enlarging the chip area. What limits the performance of integrated circuits today are the interconnections and packaging related issues. This is true for CMOS, bipolar, and gallium arsenide systems. Interconnections and packaging will gain even more importance as the sizes

of transistors are further decreased. Interconnections play an important role in determining the speed, area, reliability, and yield of very large-scale integrated (VLSI) circuits.

Because VLSI circuits contain many active devices, and their components interact with each other strongly, traditional circuit theory is unable to adequately handle the analysis. It becomes necessary to include the interconnect when modeling the active devices on a board. An interconnect is a featureless signal path at low frequencies. The connectivity and characteristics of devices and components determine the circuit operation. However, at high frequencies the interconnects become components themselves [6].

When the interconnections are sufficiently long or the circuits are sufficiently fast such that the length of the line is on the order of the signal wavelength, the interconnects must be modeled as transmission lines. This is the case at the package level for all IC technologies. To obtain accurate chip-to-chip delay and cross-talk noise estimates, bonding wires, package pins, and board interconnections should be modeled as transmission lines. At the board level, significant reflections can be generated from the end of the line and from capacitive and inductive discontinuities due to connectors, package pins, vias, and corners in board wiring [7].

CHAPTER 3

TRANSMISSION LINE THEORY

3.1 The Distributed Circuit Topology

In order to analyze a transmission line, regardless of the structure (microstrip, coaxial, wire above ground) in terms of ac circuit theory, it is necessary to obtain the equivalent circuit of the line. Since any passive network can be composed only of a combination of resistive, capacitive, and inductive elements, the final circuit must contain only combinations of these. One restriction placed on our equivalent circuit is that the length of each subsection must be much smaller than the wavelength of the applied frequency, so that each subsection can be considered a circuit and the elements within the subsection can be precisely defined. When many subsections are cascaded together to form an infinitely long line, ac analysis can be applied to each individual subsection.

To determine the equivalent circuit for a small subsection of transmission line, a voltage can be applied to the input terminals of the transmission line. It becomes evident that the voltage at the output end of the small subsection is smaller than the input voltage, and indicating a resistive voltage drop through the transmission line. Thus, the small subsection must have a series resistance component in the equivalent circuit.

If the voltage across the line is not changing with time, then it becomes apparent that the voltage can be supported only by a static electric field, since $V = \int E \cdot dl$. The presence of an electric field requires that there be free charges of opposite polarity

on the two conductors of the transmission line, since static electric field can arise only from such free charges. The free (stored) charge, accompanied by a voltage, represents a capacitor since $C = q/V$. Thus, the equivalent circuit for the small subsection must also contain capacitive component.

In addition to the static electric field present between the conductors, there is a magnetic field or flux as a result of the current flow as given by Ampere's law. If the magnetic flux linking the two conductors is changing with time, then the voltage at the input and output terminals of the transmission line will vary not only by the resistive drop described above, but also by the induced voltage. A voltage drop is induced from the time-changing flux. This time-changing flux is identified as an inductance. Thus, the equivalent subsection must contain an inductive component for the subsection of the line.

One further equivalent circuit component that remains to be identified is that associated with any current flow across the insulator between the conductors. Such a current flow can result from ordinary conduction through the insulator, or can result from losses associated with time changing electric and magnetic fields. Generally speaking, the electric conduction for common insulators used in transmission lines is very small and can be neglected. In the event that this is not true, and in order to be complete, this effect is included in the equivalent circuit model. Since both insulator conduction and other loss terms represent a current flow between the conductors which is in phase with the voltage, this loss can be represented by a shunt resistor between the conductors.

Thus, the equivalent circuit depicted by Figure 3.1 contains a series resistance, series inductance, shunt capacitance, and shunt resistance. These parameters are always taken as per-unit-length values.

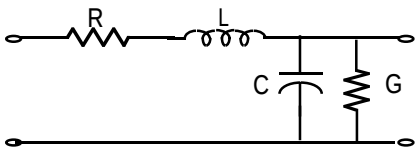

Figure 3.1: Complete equivalent circuit for a single subsection of transmission line.

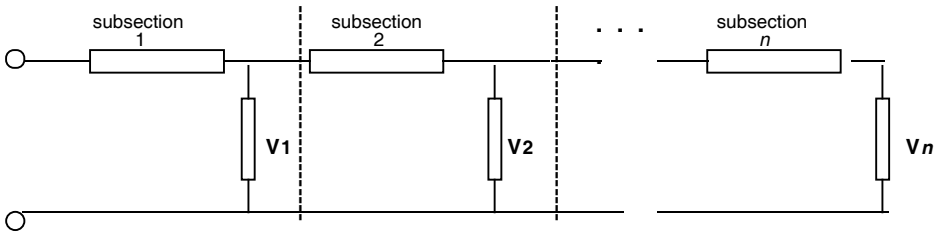

Figure 3.2: Cascaded lumped sections represent entire length of transmission line.

3.2 The Propagation Constant and Impedance of an Ideal Transmission Line

The entire length of transmission line may be modeled as a cascade of the lumped equivalent circuits, where the subsections are labeled 1 through n as shown in Figure 3.2.

It is apparent that the ratio of the input voltage to the voltage at the nth section is

$$\frac{V_o}{V_n} = \frac{V_o}{V_1} \cdot \frac{V_1}{V_2} \cdot \frac{V_2}{V_3} \cdots \frac{V_{n-1}}{V_n} \tag{3.1}$$

The total propagation of n cascaded sections is the natural logarithm of the ratio of input to output voltage or the natural logarithm of Equation (3.1). Taking the logarithm of both sides results in

$$\ln \frac{V_o}{V_n} = \ln \frac{V_o}{V_1} + \ln \frac{V_1}{V_2} + \ln \frac{V_2}{V_3} + \cdots + \ln \frac{V_{n-1}}{V_n} \tag{3.2}$$

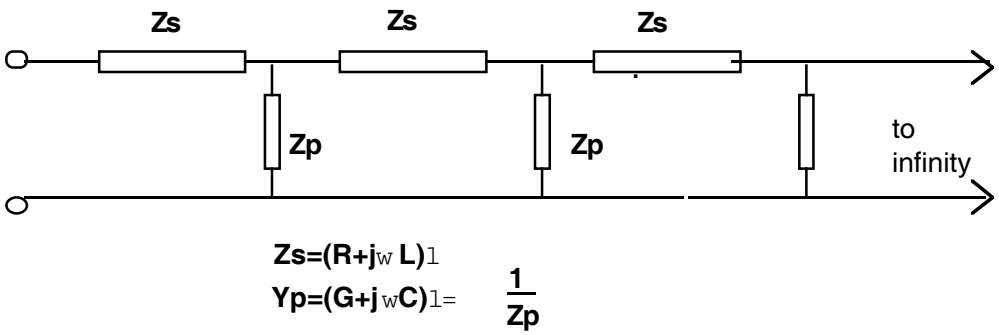

Figure 3.3: Infinite cascade of subsections.

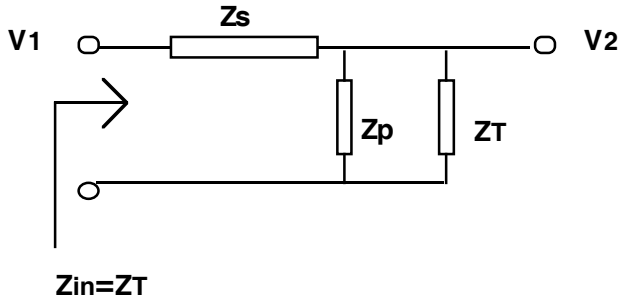

Figure 3.4: Equivalent impedance.

or

$$\gamma_T = \gamma_1 + \gamma_2 + \gamma_3 + \cdots + \gamma_n = n\gamma_1 \tag{3.3}$$

Thus, the phase shift of n sections in series is just n times the phase shift of each individual subsection of line. Similarly, the attenuation constant is the attenuation constant of one subsection multiplied by the number of subsections.

Since the line is assumed to be infinitely long and uniform, the impedance seen looking into any subsection must be the same as that of all other subsections. Thus, Figure 3.3 can be simplified to the form of Figure 3.4 where Z_T is the characteristic impedance of the line and Z_{in} must equal Z_T.

It is easily seen that

$$Z_{in} = Z_s + \frac{Z_p Z_T}{Z_p + Z_T} \tag{3.4}$$

and solving for Z_T

$$Z_T = \frac{Z_s \pm \sqrt{Z_s^2 + 4Z_s Z_p}}{2} \tag{3.5}$$

substituting Z_s and Y_p in Equation 3.5,

$$Z_T = \frac{1}{2} l(R + j\omega L) \pm \frac{1}{2}\sqrt{l^2(R + j\omega L)^2 + 4\frac{R + j\omega L}{G + j\omega C}} \tag{3.6}$$

since $l \ll 1$, all the parameters lR, lL, lG, and lC decrease in the same proportion since R, L, G, and C are constant. The subsection size l can be reduced sufficiently so that both terms $(R + j\omega L)l$ are negligible compared to the constant ratio, and then Equation (3.6) becomes

$$Z_T = \sqrt{\frac{R + j\omega L}{G + j\omega C}} = \sqrt{Z_s Z_p} = \sqrt{\frac{Z_s}{Y_p}} \tag{3.7}$$

which represents a simple expression for the characteristic impedance of the general line where the losses are not small. It can be seen that this impedance will vary with the applied frequency.

Referring to Figure 3.4, the propagation constant can be defined as the ratio of the input to output voltage.

$$V_2 = V_1 \frac{Z_T Z_p}{Z_T + Z_p} \frac{1}{Z_s + \frac{Z_T Z_p}{Z_T + Z_p}} \tag{3.8}$$

Multiplying and collecting terms

$$\frac{V_1}{V_2} = 1 + \frac{Z_s}{Z_p} + \frac{Z_s}{Z_T} \tag{3.9}$$

where $Z_T = \sqrt{Z_s Z_p} = \sqrt{\frac{R + j\omega L}{G + j\omega C}}$ and

$$\gamma_l = \alpha_l + j\beta l = \ln(\frac{V_1}{V_2}) = \ln(1 + Z_s(\frac{1}{Z_p} + \frac{1}{Z_T})) \tag{3.10}$$

Substituting Z_T from Equation (3.7) and Y_p for $\frac{1}{Z_p}$ results in

$$\gamma_l = \ln(1 + Z_s(Y_p + \sqrt{\frac{Y_p}{Z_s}})) \tag{3.11}$$

Allowing the subsection l to become small enough so that Y_p becomes negligible compared to $\sqrt{\frac{Y_p}{Z_s}}$ reduces Equation (3.11) to

$$\gamma_l = ln(1 + Z_s\sqrt{\frac{Y_p}{Z_s}}) = ln(1 + \sqrt{Z_s Y_p}) \tag{3.12}$$

Making use of the natural logarithm identity

$$\ln(1 + \nu) = \nu - \frac{\nu^2}{2} + \frac{\nu^3}{3} \cdots etc \tag{3.13}$$

which is approximately equal to ν for small ν, Equation 3.11 becomes

$$\gamma_l = \sqrt{Z_s Y_P} - \frac{Z_s Y_P}{2} + \cdots etc. \tag{3.14}$$

Since $l \ll 1$, then $\sqrt{Z_s Y_p} \ll 1$, so that the higher-order terms in Equation (3.12) can be neglected to yield:

$$\gamma_l = \sqrt{Z_s Y_p} = l\sqrt{(R + j\omega L)(G + j\omega C)} \tag{3.15}$$

for each subsection. The propagation constant per unit length is thus:

$$\gamma = \frac{\gamma_l}{l} = \sqrt{(R + j\omega L)(G + j\omega C)} \tag{3.16}$$

with all parameters taken per unit length.

3.3 Differential Equations and Transmission Line General Theory

Analysis of transmission line in terms of simple ac theory provides some physical insights and understanding of the fundamental behavior of such lines. For more

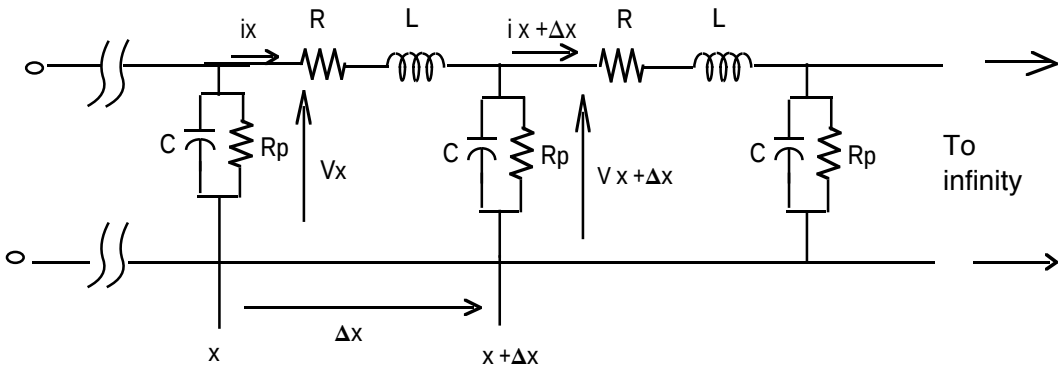

Figure 3.5: The ac circuit topology for transmission lines.

advanced cases, transmission-line theory using ac theory becomes too complicated and it becomes more convenient and useful to treat such lines in terms of differential equations, which develop into the wave equation.

Assuming the same R, L, G, and C as in the ac circuit topology, the differential equations are obtained for the transmission line. Variables R, L, G, and C are again taken as per-unit length values. The voltages and currents are sinusoidal and at any point x, the time variation of voltage is $v_x = v_o e^{j\omega t}$.

Applying Kirchoff's laws to Figure 3.5

$$v_{x+\Delta x} - v_x = -i_x(R + j\omega L)\Delta x \tag{3.17}$$

and

$$i_{x+\Delta x} - i_x = \frac{v_{x+\Delta x}}{R_p \Delta x} + \frac{v_{x+\Delta x}}{1/j\omega C \Delta x} \tag{3.18}$$

Letting $1/R_p = G$, the conductance per unit length, Equation (3.18) becomes

$$i_{x+\Delta x} - i_x = -v_{x+\Delta x}(G + j\omega C)\Delta x \tag{3.19}$$

Note that $v_{x+\Delta x} - v_x$ and $i_{x+\Delta x} - i_x$ are just the incremental voltages and current drops respectively along the line. Dividing both sides of Equation (3.17) and (3.18)

by Δx yields $\frac{\Delta v_x}{\Delta x} = -i_x(R + j\omega L)$ and $\frac{\Delta i_x}{\Delta x} = -v_x(G + j\omega C)$. Now, if the incremental distance Δx becomes very small, then the incremental voltage or current change per incremental distance becomes the derivative. The following two fundamental differential equations for a uniform transmission line are thus derived:

$$\frac{dv_x}{dx} = -(R + j\omega L)i_x \tag{3.20}$$

$$\frac{di_x}{dx} = -(G + j\omega C)v_x \tag{3.21}$$

where all parameters are per unit length.

Taking the second derivative of the above equations with respect to x and substituting one in the other,

$$\frac{d^2v_x}{dx^2} = (R + j\omega L)(G + j\omega C)v_x = \gamma^2 v_x \tag{3.22}$$

and

$$\frac{d^2i_x}{dx^2} = (R + j\omega L)(G + j\omega C)i_x = \gamma^2 i_x \tag{3.23}$$

where

$$\gamma^2 = (R + j\omega L)(G + j\omega C). \tag{3.24}$$

One possible solution to these equations is

$$v_x = v_A e^{-\gamma x} + v_B e^{\gamma x} \tag{3.25}$$

$$i_x = i_A e^{-\gamma x} + i_B e^{\gamma x} \tag{3.26}$$

where γ is as previously defined, and the coefficients are determined by the boundary conditions of the line. Since i_A and i_B are related to v_A and v_B, Equation (3.26) can be simplified to

$$i_x = \sqrt{\frac{G + j\omega C}{R + j\omega L}}(v_A e^{-\gamma x} v_B e^{\gamma x}) \tag{3.27}$$

It should be noted that the sinusoidal variations of current and voltage were assumed in the derivation of the above equations. If the sinusoidal variation is represented explicitly these equations become

$$v_x = e^{j\omega t}(v_A e^{-\gamma x} + v_B e^{\gamma x}) \tag{3.28}$$

$$i_x = e^{j\omega t}\sqrt{\frac{G + j\omega C}{R + j\omega L}}(v_A e^{-\gamma x} v_B e^{\gamma x}) \tag{3.29}$$

3.4 Characteristic Impedance of a Uniform Line

The impedance at a point x on the transmission line is equal to the ratio of the voltage divided by the current at that point. This ratio can be obtained from Equation (3.20) along with the general solution given by Equations (3.28) and (3.29). From Equation (3.20)

$$i_x = -\frac{1}{R + j\omega L}\frac{dv_x}{dx} \tag{3.30}$$

The derivative on the right side can be obtained from Equation (3.28)

$$\frac{dv_x}{dx} = (-\gamma v_A e^{-\gamma x} + \gamma v_V e^{\gamma x})e^{j\omega t} \tag{3.31}$$

Substituting this into Equation (3.30) results in

$$i_x = \frac{-\gamma}{R + j\omega L}(-v_A e^{-\gamma x} + v_B e^{\gamma x}) \tag{3.32}$$

The impedance is defined as the ratio of voltage to current at a given point:

$$Z_o = \frac{v_x}{i_x} = \frac{v_A e^{-\gamma x} + v_B e^{\gamma x}}{-v_A e^{-\gamma x} + v_B e^{\gamma x}}\frac{R + j\omega L}{-\gamma} \tag{3.33}$$

If the line is assumed to be infinitely long, then it is necessary that the constant v_B be equal to zero; otherwise, as x becomes large, the terms with positive exponents become very large. This is equivalent to stating there are no waves traveling in the

negative x direction. Setting $v_B = 0$ and canceling appropriate terms, the impedance becomes:

$$Z_o = \frac{R + j\omega L}{\gamma} = \sqrt{\frac{R + j\omega L}{G + j\omega C}} \tag{3.34}$$

This is known as the characteristic impedance of the line, since it is dependent on the characteristic parameters R, L, G, and C. It can be seen that for this general case the impedance is complex, containing resistive and reactive components. It is a function of the applied frequency, approaching a constant value of $\sqrt{L/C}$ for high frequency, assuming that all parameters are frequency-independent (which is not usually the case. The real part of γ gives the reduction in voltage or current along the line. This quantity, when evaluated per unit length of line, is referred to as the attenuation constant:

$$\alpha = Re(\gamma) = Re(\sqrt{(R + j\omega L)(G + j\omega C)}.) \tag{3.35}$$

Thus, the propagation constant can be expressed as the sum of the attenuation and phase constant:

$$\gamma = \alpha + j\beta \tag{3.36}$$

If it is assumed that the losses are small but not necessarily negligible, i.e., $R \ll \omega L$ and $G \ll \omega C$, the attenuation and phase constants can be approximated as

$$\alpha = \frac{R}{2\sqrt{L/C}} + \frac{G}{2}\sqrt{\frac{L}{C}} \tag{3.37}$$

and

$$\beta = \omega\sqrt{LC}(1 + \frac{R^2}{8\omega^2 L^2} + \frac{G^2}{8\omega^2 C^2} - \frac{RG}{4\omega^2 LC}) \tag{3.38}$$

If the line has small losses, β reduces to $\approx \omega\sqrt{LC}$.

3.5 Dispersion in Material

In dispersive lines, the propagation constant is frequency dependent. Ambiguity concerning the velocity of propagation of a signal stems primarily from the phenomenon of dispersion. When no dispersion is present, there are no losses, none of the parameters are frequency-dependent, and the group and phase velocities are identical. The phase velocity is easily found to be $\nu = \omega/\beta$, while the group velocity is $u = \frac{1}{\frac{d\beta}{d\omega}}$. The phase velocity decreases with increasing frequency. The index of refraction, initially defined for optical materials is

$$\eta = c/\nu \tag{3.39}$$

The index of refraction is proportional to the reciprocal of the phase velocity. The index of refraction η increases with frequency, while the phase velocity decreases with frequency. This situation has become known as "normal" dispersion. It is possible for the index of refraction to decrease with frequency, thus have an increasing phase velocity. Since such materials differ from the normal case, they were arbitrarily classified as anomalous. In general, anomalous dispersion is much more common than normal dispersion. For most nonmagnetic materials, the index of refraction is

$$\eta = \sqrt{\epsilon}_r \tag{3.40}$$

where ϵ_r is the dielectric constant. It is well known that, in general, the dielectric constant of materials decreases with increasing frequency, eventually approaching that of free space. The dielectric constant, however, is not well behaved throughout the entire frequency spectrum; rather, the same value can exist for several different frequencies as a result of absorption bands. In some cases a material cannot be classified as either anomalous or normal because the dielectric constant may increase and decrease through the frequency spectrum. In an anomalously dispersive medium,

the group velocity is greater that the phase velocity. A metal, or any material with relatively large conductivity through which an electromagnetic wave is propagating, is generally considered to exhibit anomalous dispersion.

It should be noted that even though conductors may satisfy the requirement of $d\nu/d\omega > 0$ for anomalous dispersion, a wave propagating in such a medium will undergo severe distortion due to the large attenuation factor α. Each frequency component will experience a different amount of attenuation so that the voltage at a large distance from the input terminals may bear no resemblance to the applied voltage. For such cases, the group velocity cannot be determined and must therefore be limited to distances for which the total attenuation is not significant.

If a signal consisting of a low-frequency and high-frequency component goes through a dispersive line, the line will exhibit either normal or anomalous dispersion. If the higher frequency travels with a slower phase velocity than the lower frequency, the dispersion is said to be normal and the group velocity of the envelope is less than the phase velocity of the carrier wave. If the higher frequency travels faster that the lower frequency, the group velocity exceeds the phase velocity and the dispersion is termed anomalous.

3.6 Skin Effect

As a pulse propagates on a real transmission line it changes shape as a result of two major sources of distortion, attenuation and dispersion. A single pulse is composed of a continuous spectrum of frequency components. If these components all propagate at the same velocity with no attenuation, they will add at any given point to produced the identical waveform. Distortion comes about when attenuation is present or when the velocity of propagation is different for the various frequencies, i.e., dispersion.

For lossy transmission lines, attenuation and dispersion are both present. In most cases, the losses are frequency dependent, which further distorts the applied pulse. There are numerous sources of both attenuation and dispersion, but for ordinary lines with applied pulses, skin effect is usually the most significant.

The finite conductivity of the conductors gives rise to a series resistance, whereas the dielectric insulator gives rise to a shunt resistance. Both of these terms will generally be frequency dependent. Even though these are absorption losses associated with the dispersion frequency range, these are usually quite small compared to the series resistance losses, so that G can usually be neglected.

All skin effect phenomena result from the fact that the current or magnetic field distribution in a conductor is frequency-dependent and also that current in any real conductor gives rise to an electric field as given by Ohm's law. The skin effect causes current to flow on the surface of a conductor, thus increasing its effective resistance. As the resistance changes, the internal inductance, due to magnetic flux penetration in the conductor, also changes.

The most fundamental way of investigating the skin effect is by applying Maxwell's equations and by finding the proper differential equations for E and H. The current and field distributions are derived by applying the boundary conditions to the transmission line. From this the attenuation and phase constant or equivalently the effective resistance and inductance can easily be determined. Similarly, Faraday's law of induced voltages and Kirchoff's voltage law can be used for the same results. This analysis, when applied to solid round wire and strip line conductors, reveals at sufficiently high frequency the resistance becomes proportional to the square root of frequency while the inductance becomes inversely proportional to the square root of frequency [8].

CHAPTER 4

TRANSMISSION LINE CHARACTERIZATION

4.1 Transmission Lines Under Test

The measurement technique developed in this study is tested on telecommunication cable and on microstrip transmission line.

The telecommunication cables tested are divided into four types. The first type is coaxial. A 50-Ω RG174 coaxial line is measured and the parameters are extracted. The Type 2 cable is composed of four insulated conductors that are not twisted. Type 3 and Type 4 are both shielded twisted pair cables. Type 3 is two twisted pairs, while Type 4 has four twisted pairs, both Type 3 and 4 are classified as AT&T category 5 cables.

The copper microstrip line is on a fiberglass substrate ($\epsilon = 4.9$), 20 cm in length, 0.13 mm in width, and the substrate is 2.1 mm above the ground plane. In order to measure the line, SMA connectors are used (see Figure 4.1). The connection discontinuity is accounted for in the measurement by adding an electrical delay to the measurements.

For the reference purposes, the five categories of telephone cables that are specified by ANSI/ICEA S-90-661-1994 standards and are defined below:

Category 1: These cables are intended for basic, voice-grade communications. Such cables are typically available in pair counts from 2 to 600.

Category 2: These cables are intended for basic, voice-grade and low speed data transmission. Their transmission characteristics are specified for frequencies up to 1

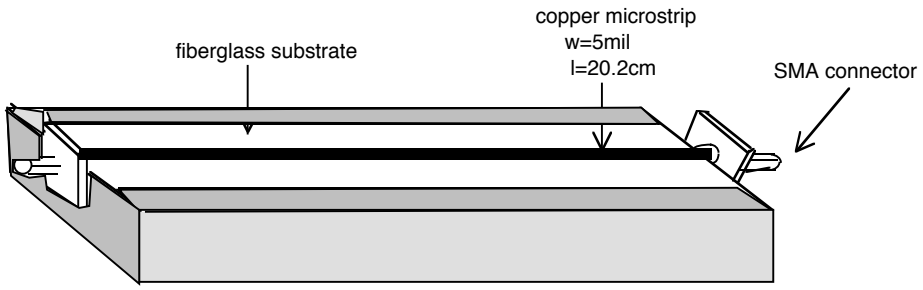

Figure 4.1: Microstrip line under test.

MHz. Such cables are typically available in pair counts from 2 to 100.

Category 3: These cables are intended for voice and data transmission. Their transmission characteristics are specified for frequencies up to 16 MHz. Such cables are typically available in pair counts from 2 to 100.

Category 4: These cables are intended for voice and data transmission. Their transmission characteristics are specified for frequencies up to 20 MHz. Such cables are typically in pair counts from 2 to 25.

Category 5: These cables are intended for voice and data transmission. Their transmission characteristics are specified for frequencies up to 100 MHz. Such cables are typically available in pair counts from 2 to 25.

4.2 Measurement Setup

Both the HP 8753 and HP 8510 Network Analyzers were used to measure the scattering parameters of the transmission lines under test. The measurement system for the scattering parameters of the transmission lines can be modeled as the two port network shown in Figure 4.2. The transmission line of length l and complex characteristic impedance Z_c is embedded between two lossless coaxial lines of impedance Z_o representing the measurement system. On the left is an RF source of an angular

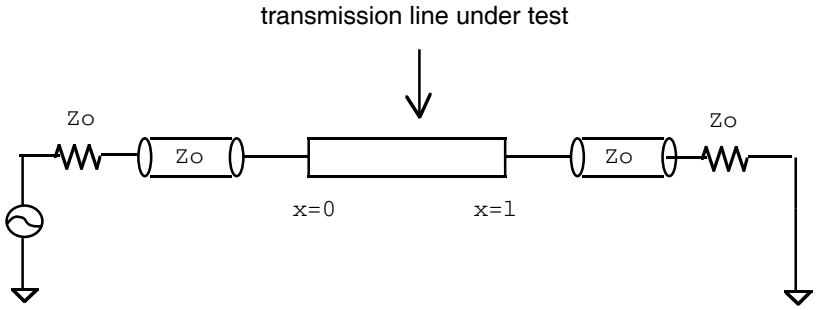

Figure 4.2: Model of measurement system.

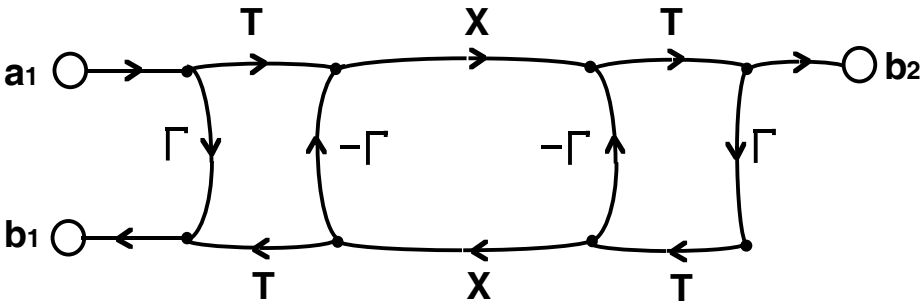

Figure 4.3: Propagating wave flow diagram.

frequency $\omega = 2\pi f$.

4.3 Wave Model Approach

The most natural method of extracting transmission line characteristic parameters from measurements is through a wave analysis of the measurement system. The measurement network, which is shown in Figure 4.2, can be represented by the signal flow diagram given by Figure 4.3. In the flow diagram, X is the complex function $X = e^{-\gamma l}$, Γ, given by $\Gamma = \frac{Z_c - Z_o}{Z_c + Z_o}$, is the reflection coefficient of the symmetric transmission line with respect to the reference system Z_o, and d is the length of the transmission line.

Applying Mason's rule to the flow diagram allows for the easy extraction of the

scattering parameters in terms traveling wave characteristics:

$$\begin{aligned} S_{11} &= \frac{\Gamma(1-X^2\Gamma^2)-\Gamma T^2X^2}{1-\Gamma^2X^2} \\ &= \frac{\Gamma-\Gamma X^2(\Gamma^2+T^2)}{1-\Gamma^2X^2} \\ &= \frac{\Gamma(1-X^2)}{1-\Gamma^2X^2} \end{aligned} \tag{4.1}$$

and

$$S_{21} = \frac{T^2X}{1-\Gamma^2X^2} \tag{4.2}$$

since the reference line is lossless, no power is dissipated along the line and $\Gamma^2+T^2 = 1$, and Equation (4.2) reduces to

$$S_{21} = \frac{(1-\Gamma^2)X}{1-\Gamma^2X^2} \tag{4.3}$$

where X is the complex function given by

$$X = e^{-\gamma l} \tag{4.4}$$

The variable Γ is the reflection coefficient of the transmission line with respect to the reference system Z_o given by

$$\Gamma = \frac{Z_c - Z_o}{Z_c + Z_o} \tag{4.5}$$

and d is the length of the transmission line.

Variables X and Γ are functions of the phase constant and the characteristic impedance, respectively. As stated in Section 3.4, the characteristic impedance of the transmission line is given by Equation (3.34), $Z_c = \sqrt{\frac{R+j\omega L}{G+j\omega C}}$, and the propagation constant as given by Equation (3.16), $\gamma = \sqrt{(R+j\omega L)(G+j\omega C)}$. Thus solving for the propagation characteristics from Equations (4.1) and (4.2), implies extracting the electrical parameters R, L, G, and C.

Taking the difference of Equations (4.1) and (4.2) and simplifying results in

$$S_{11} - S_{21} = \frac{\Gamma - X}{1 - \Gamma X} \tag{4.6}$$

Adding Equations (4.1) and (4.2) and simplifying results in

$$S_{11} + S_{21} = \frac{\Gamma + X}{1 + \Gamma X} \tag{4.7}$$

Multiplying Equations (4.6) and (4.7) results in

$$(S_{11} + S_{21})(S_{11} - S_{21}) = S_{11}^2 - S_{21}^2 = \frac{\Gamma + X}{1 + \Gamma X}\frac{\Gamma - X}{1 - \Gamma X} = \frac{\Gamma^2 - X^2}{1 - \Gamma^2 X^2} \tag{4.8}$$

Defining a quantity Q and manipulating Equations (4.8) and (4.1):

$$Q = \frac{S_{11}^2 - S_{21}^2 + 1}{2S_{11}} = \frac{\Gamma^2 + 1}{2\Gamma} \tag{4.9}$$

allows the reflection coefficient to be solved for with the following equation:

$$\Gamma = Q \pm \sqrt{Q^2 - 1} \tag{4.10}$$

Using Equation (4.7) to define the quantity U,

$$U = S_{11} + S_{21} = \frac{\Gamma + X}{1 + \Gamma X} \tag{4.11}$$

Making use of the quantity U defined above allows to solve for X in terms of U and Γ, which are both defined in terms of the scattering parameters above. As a result of the above manipulations, both Γ and X are directly extracted from the scattering parameters. The values for L, R, G and C can then be extracted using Equations (4.4), (4.5), and the following:

$$R = Re[Z_c \cdot \gamma] \tag{4.12}$$

$$L = \frac{Im[Z_c \cdot \gamma]}{\omega} \tag{4.13}$$

$$C = \frac{Im[\gamma / Z_c]}{\omega} \tag{4.14}$$

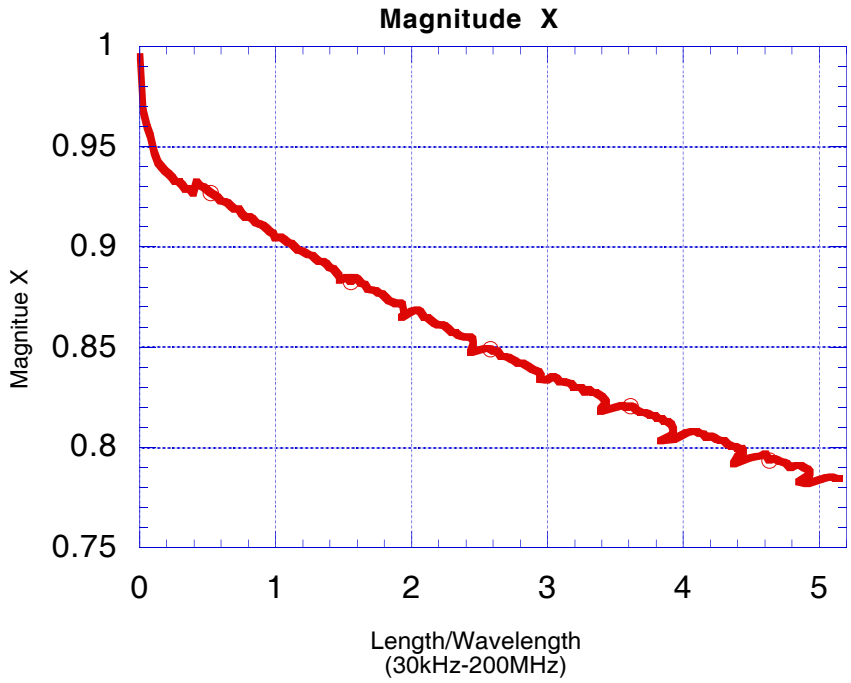

Figure 4.4: Magnitude of X verses the length of the line normalized to a wavelength for the 50-Ω coaxial cable.

$$G = Re[\frac{\gamma}{Z_c} \tag{4.15}$$

The 50-Ω coaxial line of length $l = 5$ m is the first transmission line to undergo this extraction. The other transmission lines follow. The scattering parameters for the 50-Ω coaxial line are measured on the HP 8753 Network Analyzer and shown in Figure 4.8 and Figure 4.9. Using the above technique, the magnitude of X is extracted with the measured scattering parameters and plotted against the length of the line normalized to a wavelength in Figure 4.4.

It becomes evident that a problem arises every half wavelength when Figure 4.5, displaying the magnitude of Γ, is examined. The "jumps" in the magnitude of Γ reappear in the characteristic impedance $Z_c = Z_o\frac{1+\Gamma}{1-\Gamma}$, as is revealed in Figure 4.6. If these "jumps" in the magnitude are ignored, then the problem carries over into the

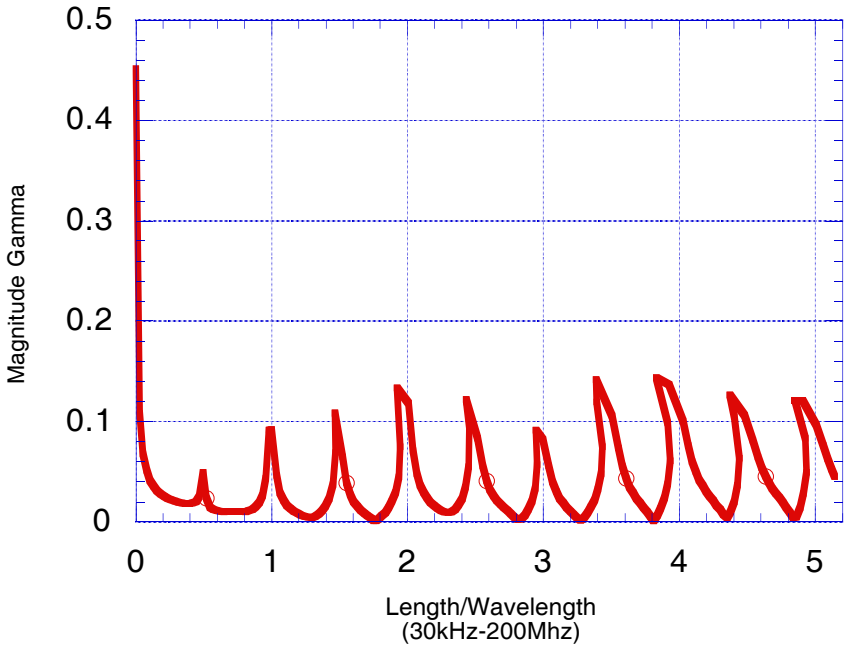

Figure 4.5: Magnitude of Γ verses the length of the line normalized to a wavelength for the 50-Ω coaxial cable.

extracted L, R, G and C which are derived from Equations (4.12)-(4.15). In Figure 4.7 the resistance "jumps" when the length of line is a half-wave multiple. This is also true for the inductance, capacitance, and conductance. The rough curve for the characteristic impedance causes the spikes in the L, R, C, and G parameters.

The cause of these "spikes" may be realized once the scattering parameters are taken under a closer inspection. It becomes evident that S_{11} goes close to zero every half wavelength, which would be expected by simple transmission theory. The impedance at any point along the line repeats every half wavelength.

Figures 4.8 and 4.9 are the measured S_{11} and S_{21} of the 50-Ω coaxial cable. It should be noted that Figure 4.8 has a very narrow magnitude range on the vertical axis because the cable is virtually a perfect match (50-Ω). Looking at Figure 4.8, the magnitude of S_{11} approaches zero every half wavelength, this causes Q in Equation

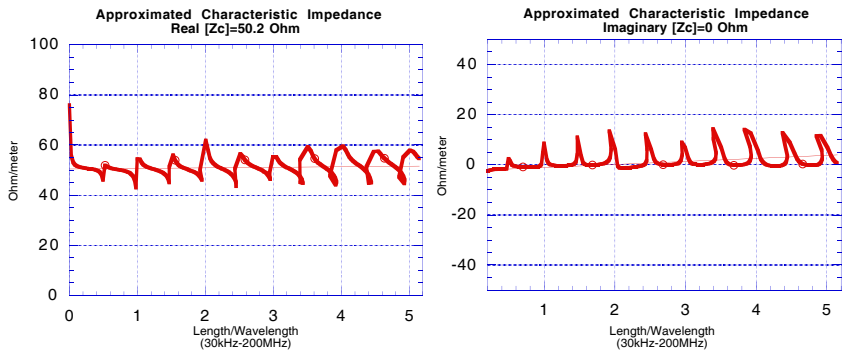

Figure 4.6: The real and imaginary parts of the characteristic impedance Z_c verses the length of the line normalized to a wavelength for the 50-Ω coaxial cable.

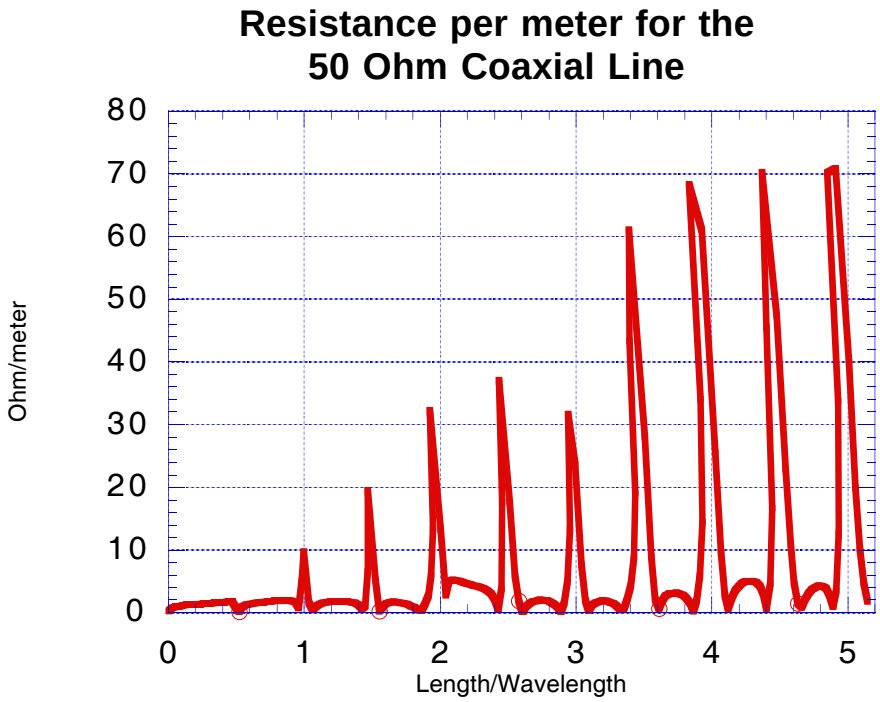

Figure 4.7: The resistance of the 50-Ω coaxial line is plotted against the length of the line normalized to a wavelength over a frequency range of 30 kHz to 200 MHz.

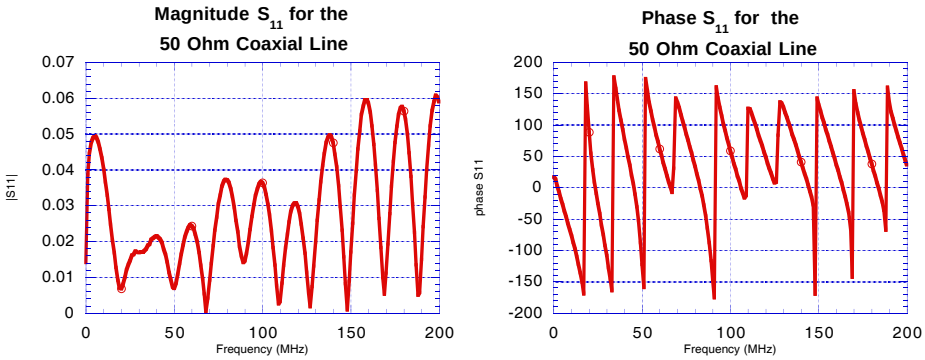

Figure 4.8: Magnitude and phase of S_{11} for the 50-Ω coaxial cable from 30 kHz to 200 MHz.

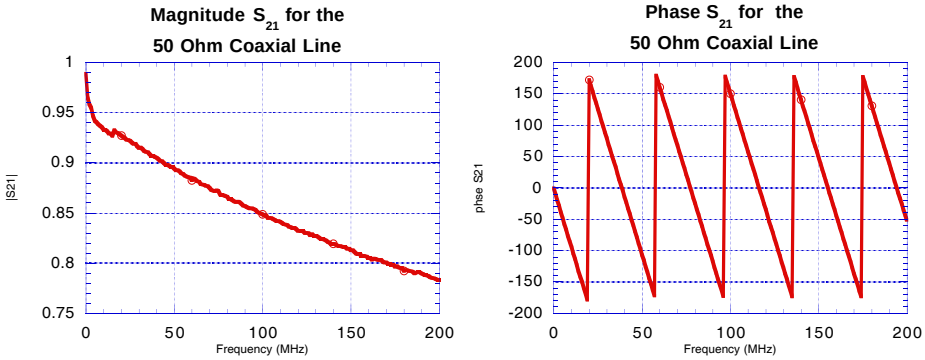

Figure 4.9: Magnitude and phase of S_{21} for the 50-Ω coaxial cable from 30 kHz to 200 MHz.

(4.9), to have singular points at these frequencies as is shown in Figure 4.25 on page 45. Unfortunately the main cause of the problem is the sensitivity of the network analyzer. It is not capable of measuring the exact values for S_{11} when the magnitude becomes very small. Since Γ is dependent on Q, the measured data points around the frequencies near half wave multiples do not allow for the extraction of the L, R, C, and G parameters, which is demonstrated in Figure 4.7, as the resistance is plotted against length normalized to a wavelength. It becomes obvious the resistance "blows up" every half-wave multiple.

In order to obtain adequate information to recover the characteristic impedance and γ from X, it becomes necessary to avoid these half-wave points. It is certainly possible to extract the transmission line parameters in the low-frequency range where the length of the line is less than a half wavelength. The results shown in Figures 4.10-4.14 give the parameters for the coaxial 50-Ω cable, lines Type 2-4, and the microstrip line. With the L, R, C, and G parameters, the velocity of propagation is derived as $v_p = \frac{1}{\sqrt{LC}}$.

4.4 ABCD Parameters

If the transmission line characterization is desired over a frequency range spanning multiple wavelengths of transmission line, it becomes necessary to find a technique to avoid these singular points at the half wavelength points when determining the lumped transmission line parameters. The first attempt at this is to avoid the division by S_{11} in Equation (4.9) by making use of the ABCD parameters as described in [9] by the following equations:

$$v_1 = Av_2 - Bi_2 \tag{4.16}$$

$$i_1 = Cv_2 - Di_2 \tag{4.17}$$

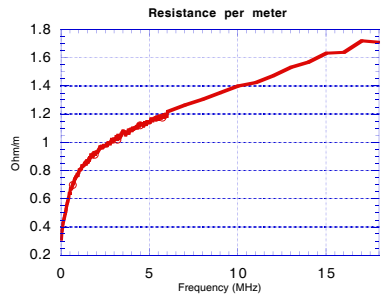

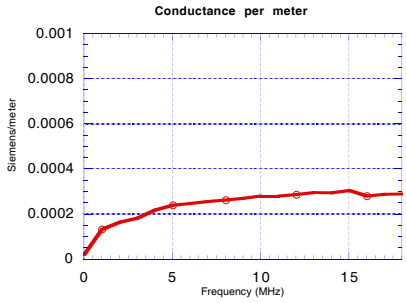

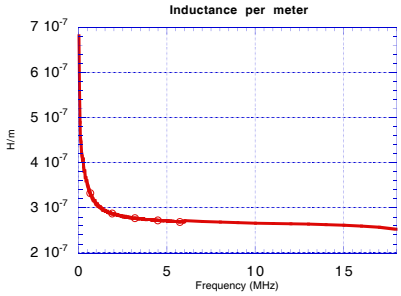

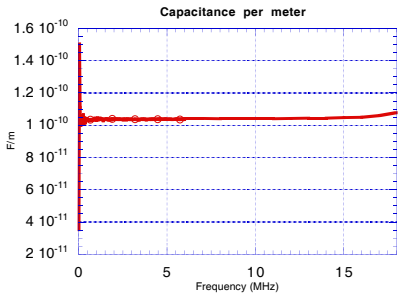

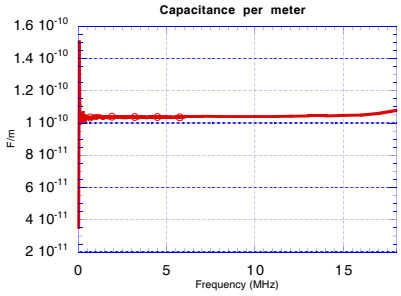

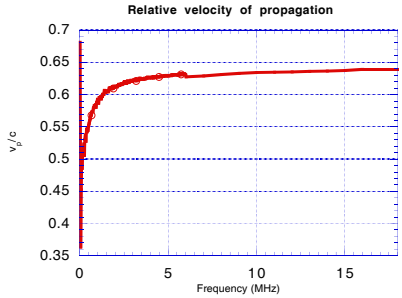

Figure 4.10: 50-Ω coaxial cable of length $l = 5$ m: LRC, v, and Z extracted with the "wave technique" up to $\lambda/2$.

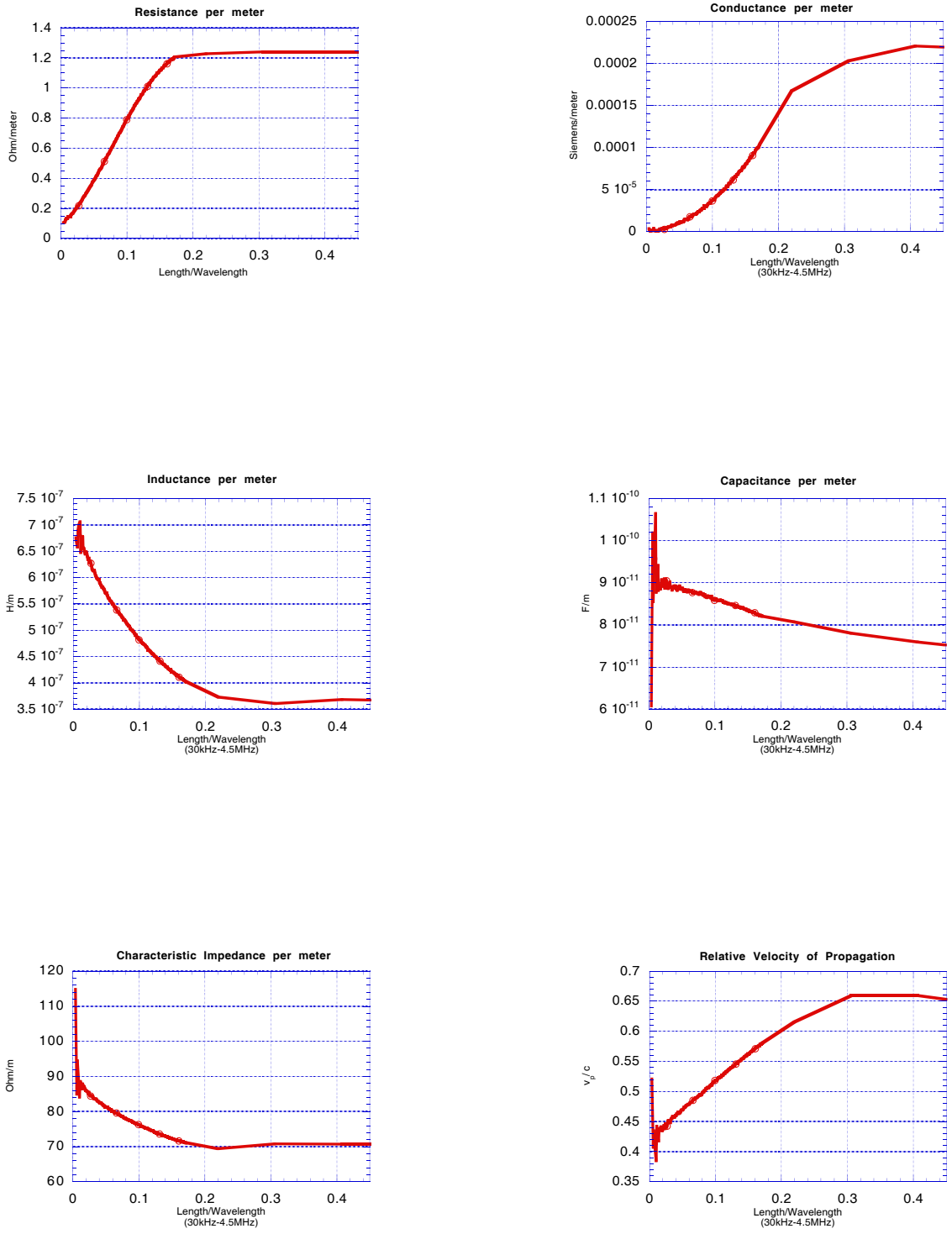

Figure 4.11: Type 2 cable of length $l = 20$ m: $LRCG$, Z, and v extracted with the "wave technique" up to $\lambda/2$.

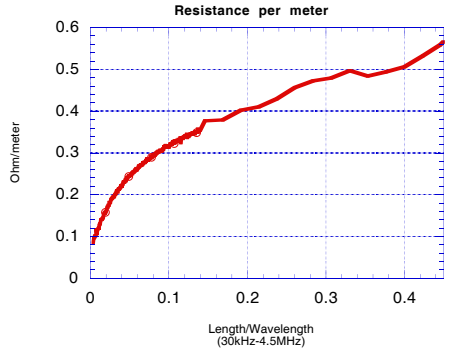

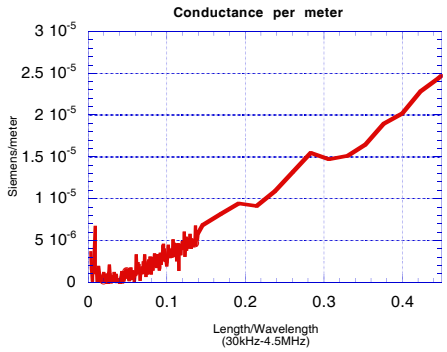

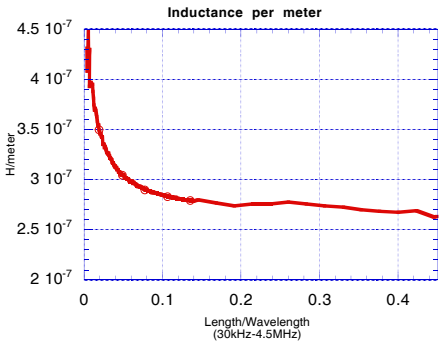

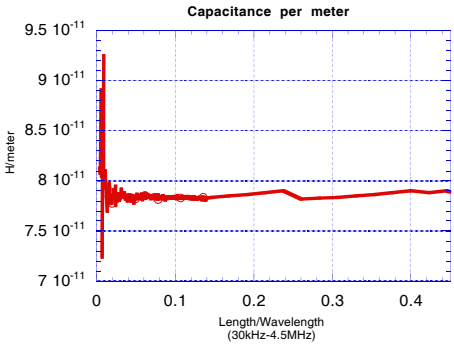

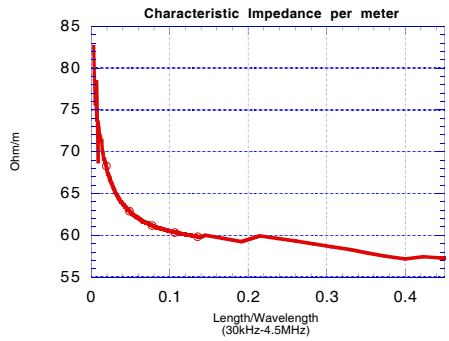

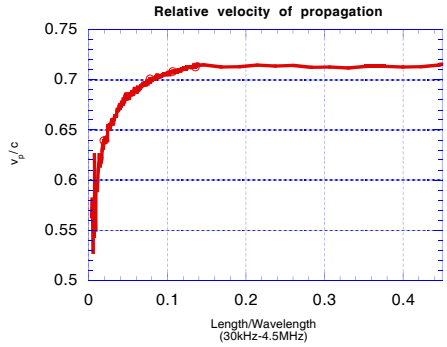

Figure 4.12: Type 3 cable of length $l = 20$ m: $LRCG$, v, and Z extracted with the "wave technique" up to $\lambda/2$.

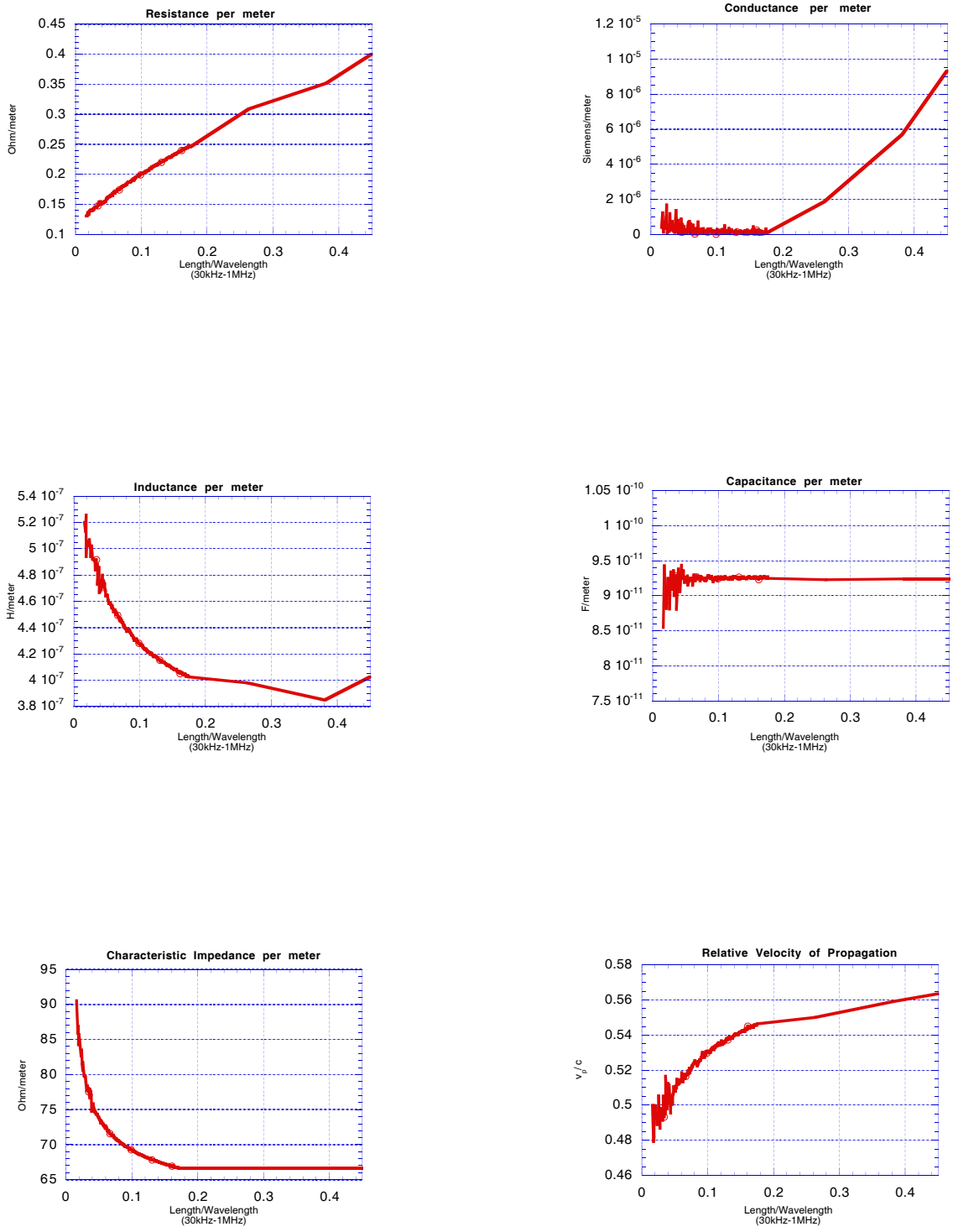

Figure 4.13: Type 4 cable of length $l = 82$ m: $LRCG$, v, and Z extracted with the "wave technique" up to $\lambda/2$.

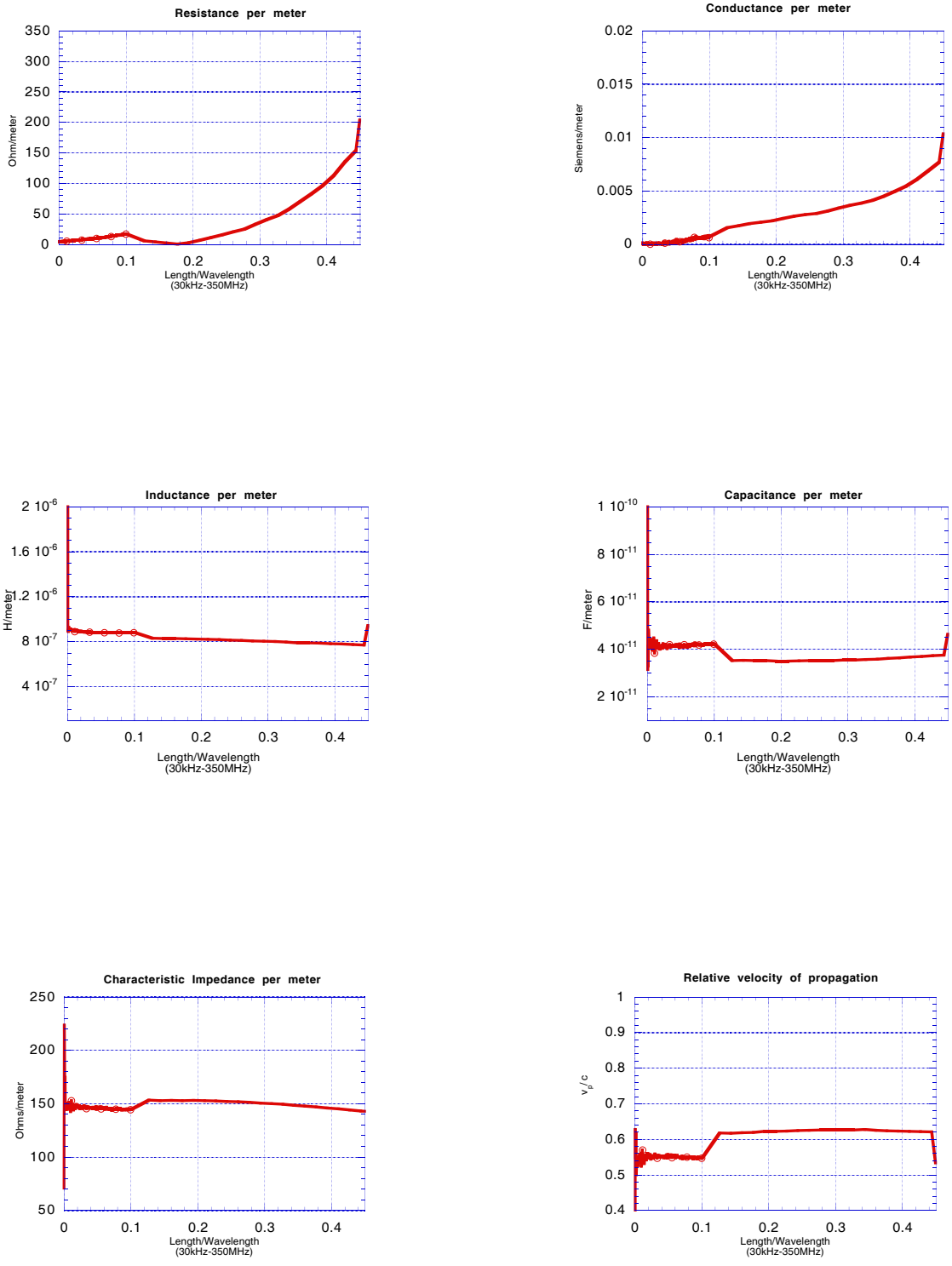

Figure 4.14: Microstrip: $LRCG$, v, and Z extracted with the "wave technique" up to $\lambda/2$.

where v_1, v_2 and i_1, i_2 are the input and output voltages and currents, respectively, of a given two port. These parameters are related to the transmission line characteristics as follows:

$$A = \cosh(\gamma d) \tag{4.18}$$

$$B = Z_c \sinh(\gamma d) \tag{4.19}$$

$$C = \frac{1}{Z_c} \sinh(\gamma d) \tag{4.20}$$

$$D = \cosh(\gamma d) \tag{4.21}$$

The reason these parameters may appear desirable is that they make it possible to convert from the scattering parameters, which were measured, to ABCD parameter without any S_{11} division as seen in the following equations:

$$\begin{aligned} A &= \frac{(1+S_{11})(1-S_{22})+S_{12}S_{21}}{2S_{21}} \\ B &= \frac{(1+S_{11})(1+S_{22})-S_{12}S_{21}}{2S_{21}} \\ C &= \frac{(1-S_{11})(1-S_{22})-S_{12}S_{21}}{2S_{21}} \\ D &= \frac{(1-S_{11})(1+S_{22})+S_{12}S_{21}}{2S_{21}} \end{aligned} \tag{4.22}$$

It then becomes possible to extract the transmission line characteristics γ and Z_c from the ABCD parameters as is indicated by Equations (4.18)-(4.21). With γ and Z_c at hand, R, L, G, and C can be found using Equations (4.12)-(4.15). Though it seems that this manipulation would get around the singularities at the half wavelength points (since the division by zero is avoided), the problem unfortunately remains as is seen in Figure 4.15.

It is again evident that the resistance blows up when the length of a line is a half wave multiple, as it did with the full-wave technique. The characteristic impedance Z_c using this technique comes out exactly as it did in Figure 4.6. Overall, it is evident

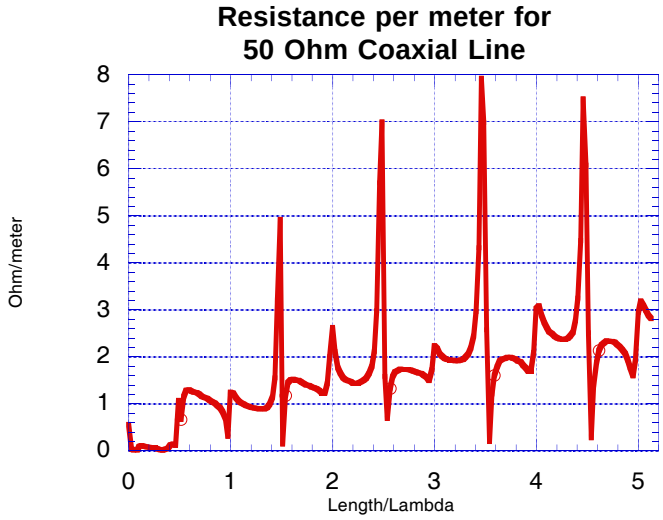

Figure 4.15: Based on the ABCD parameter technique, the resistance of the 50-Ω coaxial line is plotted against the length of the line normalized to a wavelength over a frequency range of 30 kHz to 200 MHz. Though the spikes are still evident, the magnitude is smaller than the spikes in Figure 4.7 where the resistance is extracted using the "wave" technique directly.

that the problem is caused by the limited sensitivity of the instrument for low values of S_{11}, and even though these ABCD parameters avoid the division by S_{11}, Z_c is still depenedent on the instrument sensitivity.

4.5 Lumped Model Topology

The next attempt at avoiding the singularity at half wave points is to relate the measured scattering parameters directly to resistive, capacitive, and inductive elements. This means assuming a lumped model topology which would allow for an easy analysis and determination of the scattering parameters. The analytically determined scattering parameters can then be related back to the original lumped elements. Similarly, the measured scattering parameters can be related to these lumped parameters.

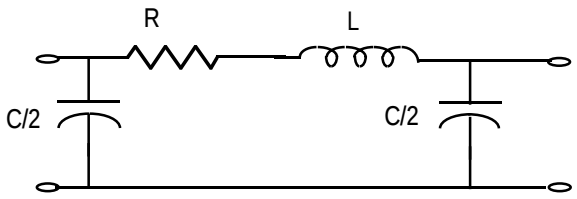

Figure 4.16: Equivalent lumped transmission line circuit.

A simple lumped topology to choose would be one similar to that depicted in Figure 3.1. The transmission line will surely have all of the parameters in the lumped topology, so why not assume this topology represents the entire length of the line? If the transmission line has a negligible conductance, the topology of Figure 3.1 can be simplified to that shown in Figure 4.16. This circuit can easily be analyzed to determine the scattering parameters. The restriction on this circuit composed of lumped elements is that the length of the subsection it represents must be much smaller than the wavelength of the applied frequency.

If the entire transmission line is represented by the lumped model, the scattering parameters of the lumped model can easily be derived as:

$$S_{11} = \frac{P - 2YZ_o - YP}{2Z_o + P + 2YZ_o + YP} \tag{4.23}$$

$$S_{21} = \frac{2Z_o}{2Z_o + P + 2YZ_o + YP} \tag{4.24}$$

where $P = (R+j\omega L)(1+\frac{j\omega CZ_o}{2})$, $Y = \frac{j\omega CZ_o}{2}$, and Z_o is the reference line characteristic impedance, as depicted in Figure 4.2. Defining a quantity $A = 2Z_o(1 - S_{21})$ allows for the extraction of Y and P given above in terms of L,R, and C lumped parameters from the given scattering parameters:

$$Y = \frac{A - 2S_{11}S_{21}Z_o - S_{11}A}{4S_{21}Z_o + 2S_{11}S_{21}Z_o + S_{11}A + A} \tag{4.25}$$

$$P = \frac{A - 2YS_{21}Z_o}{S_{21}(1 + Y)} \tag{4.26}$$

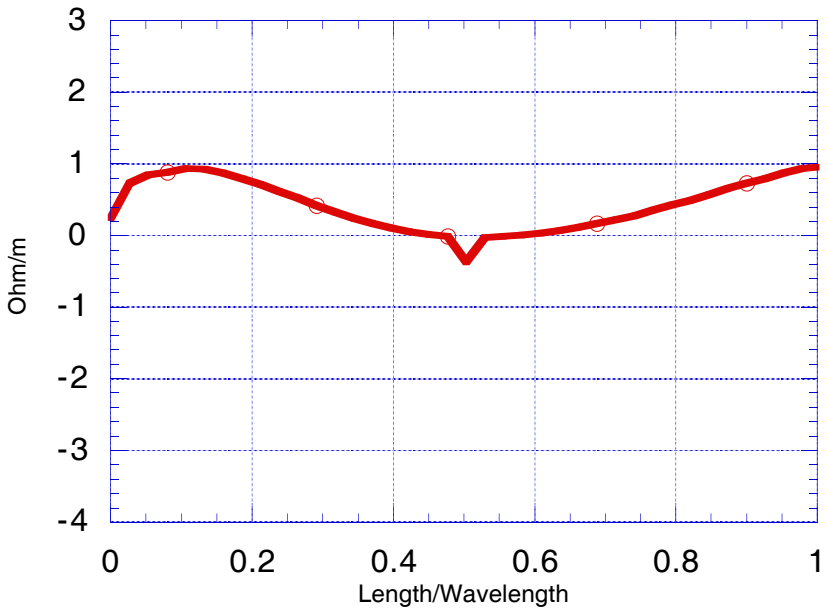

Figure 4.17: 50-Ω coaxial cable (l = 5 m) "lumped model" resistance per meter up to λ.

Now the L, R, and C parameters are derived from Y and P and are divided by the length of the line in order to get the inductive, resistive, and capacitive values per unit length. With the L, R, and C parameters, the velocity of propagation is derived $v_p = \frac{1}{\sqrt{LC}}$ and the characteristic impedance is $Z_c = \sqrt{\frac{R+j\omega L}{j\omega C}}$.

It may be of some interest to examine the exact range in which this model is valid. Theoretically the lumped model represents a length of transmission line that is much less than a wavelength. What defines "much less"? The results of an attempt made to use this lumped model in the frequency range where the length of the line reaches a wavelength are given in Figures 4.17-4.19. It becomes evident that the lumped resistance and inductance start to stray from the values determined with the wave technique and given by Figures 4.17 and 4.18 at about a 10th of a wavelength.

Zooming in on the region where the length of the line is approximately a 10th of

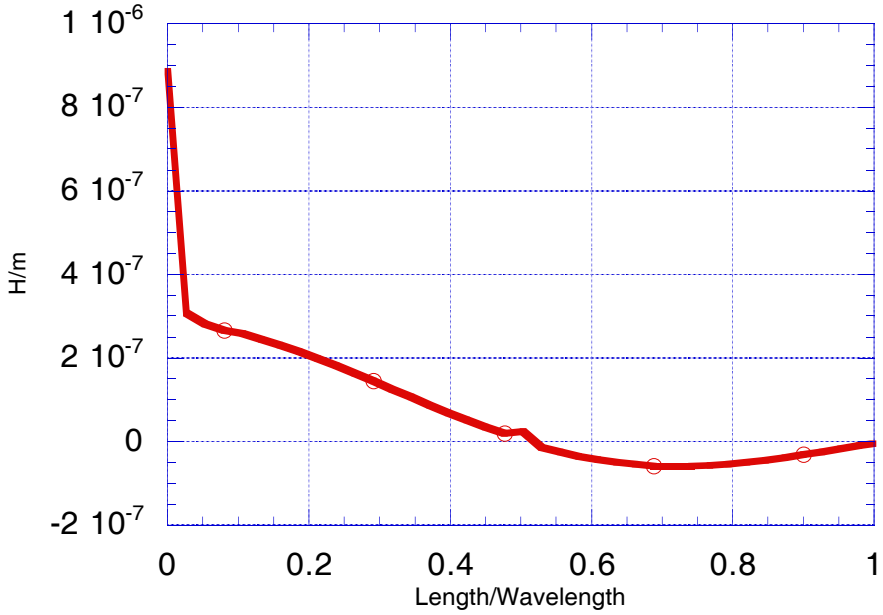

Figure 4.18: 50-Ω coaxial cable ($l = 5$ m) "lumped model" inductance per meter up to λ.

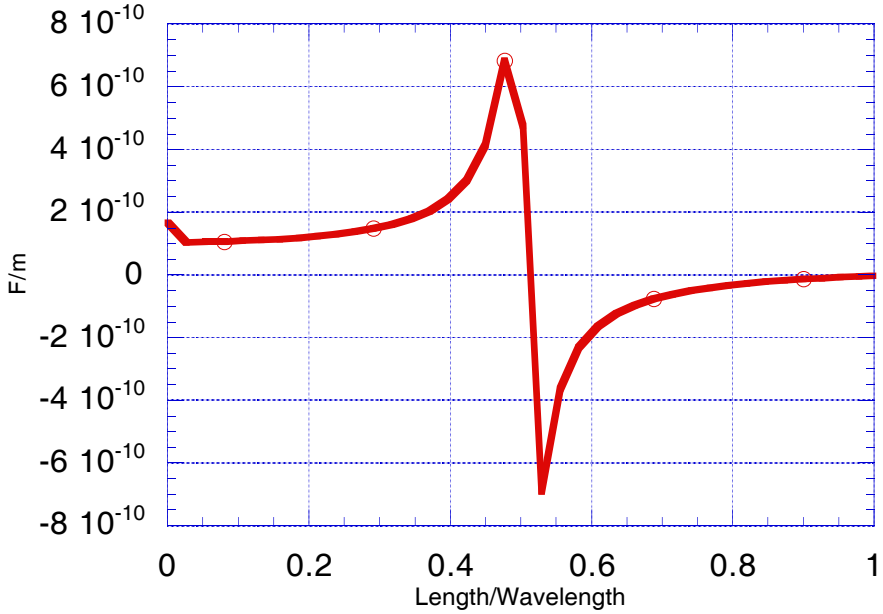

Figure 4.19: 50-Ω coaxial cable ($l = 5$ m) "lumped model" capacitance per meter up to λ.

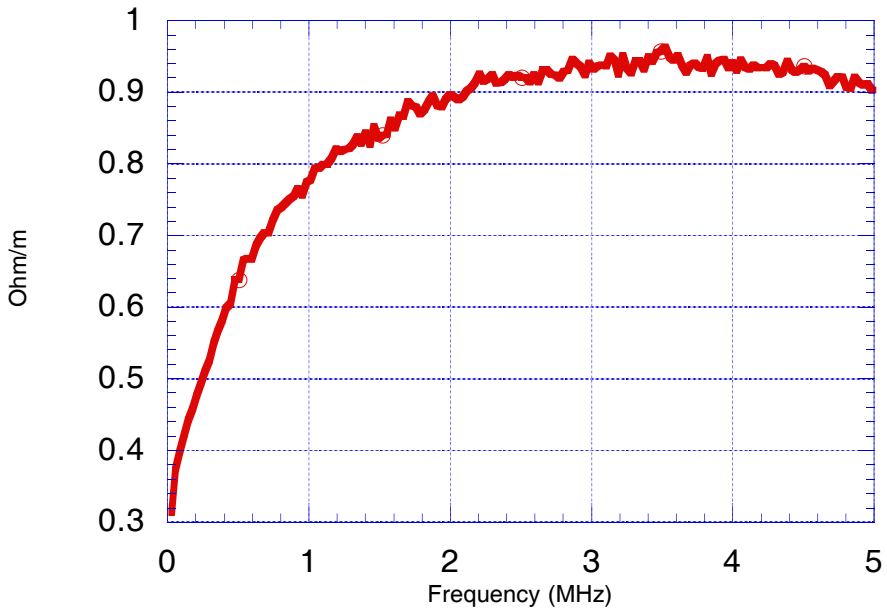

Figure 4.20: 50-Ω coaxial cable (l = 5 m) "lumped model" resistance per meter up to $\lambda/10$.

a wavelength, the lumped model methodology is employed to extract the L, R, and C parameters for the 50-Ω coaxial cable. The results for the line are shown here in Figures 4.20-4.24.

This method obviously does not add any improvement to the "wave "approach described in Section 4.3. In fact this "lumped model" is only valid in the frequency ranges where the line length is considerably less than a wavelength, around a 10th, while the "wave" approach may be used up to frequencies where the length of line approaches half a wavelength, nearly five times the frequency range of the "lumped" approach. If it is desirable to extract the characteristic parameters into higher frequencies, the lumped model does not have any advantage over the "wave" approach, because not only is the wave approach valid in a larger frequency range, but it also accounts for the conductance; thus, the "wave" appoach takes all parameters into

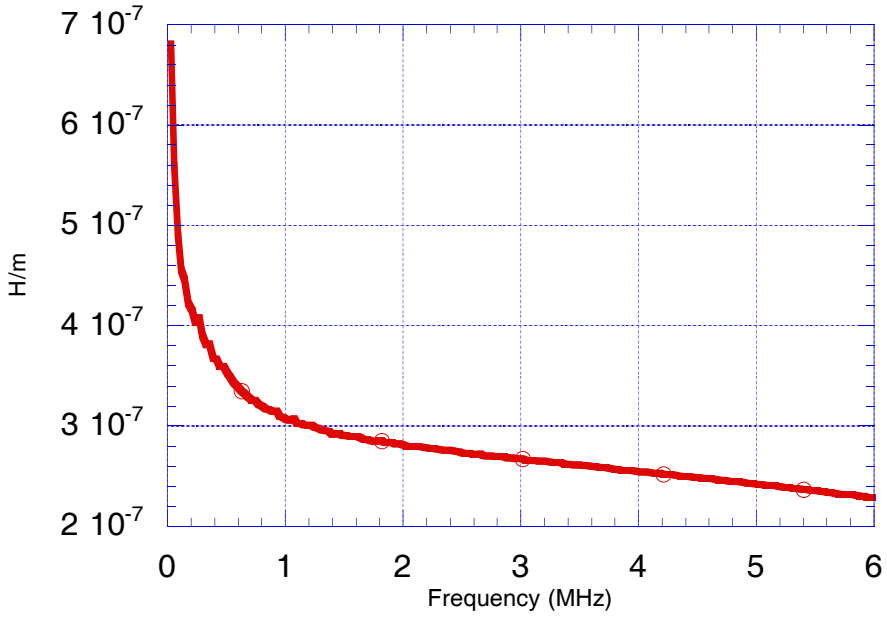

Figure 4.21: 50-Ω coaxial cable ($l = 5$ m) "lumped model" inductance per meter up to $\lambda/10$.

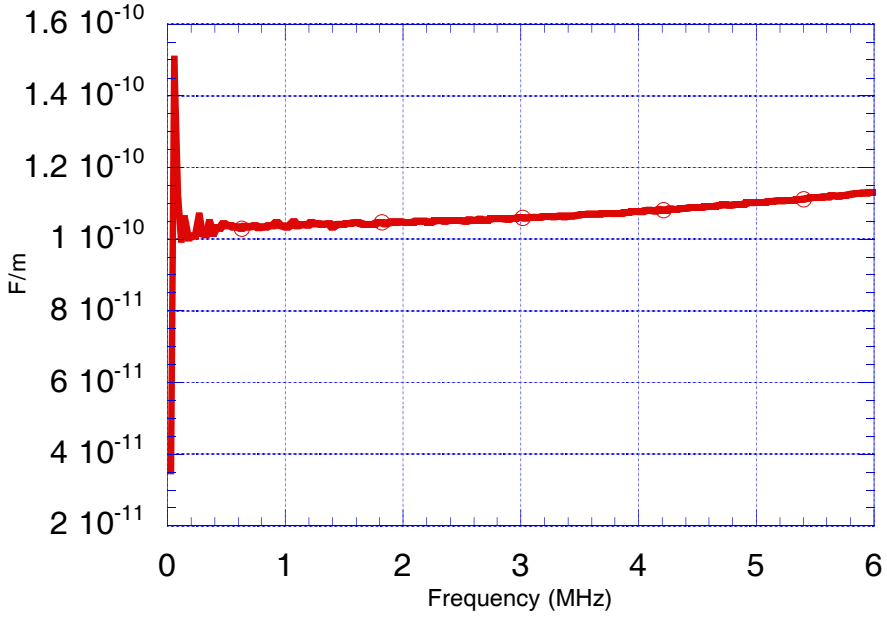

Figure 4.22: 50-Ω coaxial cable ($l = 5$ m) "lumped model" capacitance per meter up to $\lambda/10$.

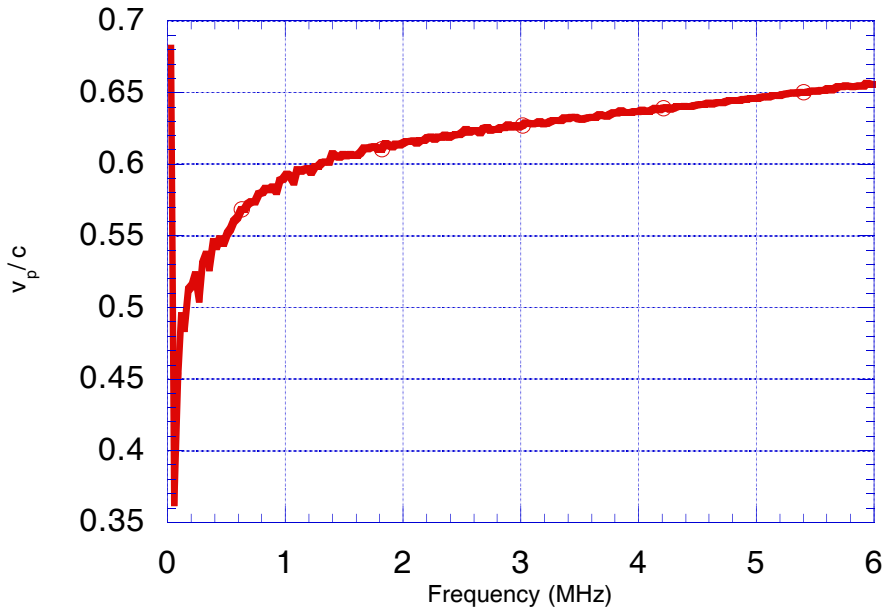

Figure 4.23: 50-Ω coaxial cable ($l = 5$ m) "lumped model" relative velocity.

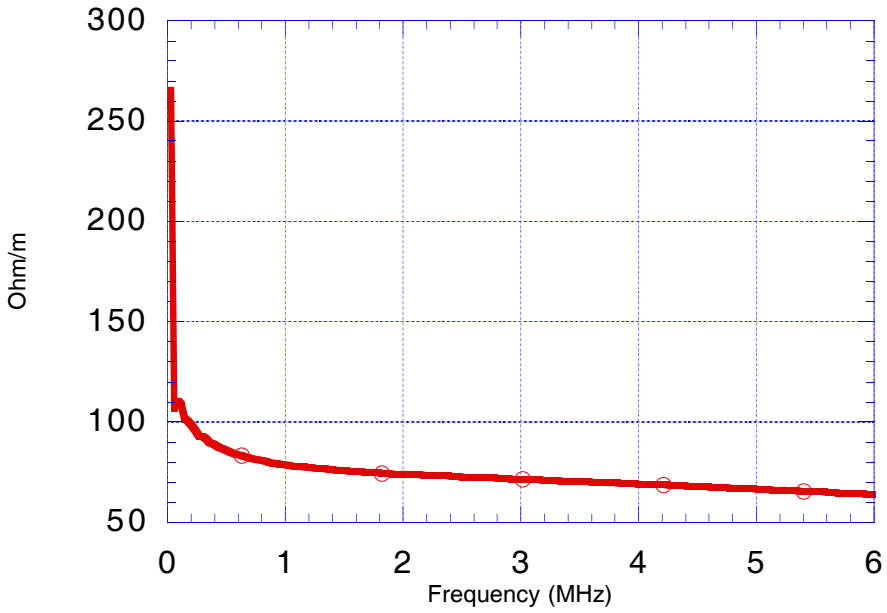

Figure 4.24: 50-Ω coaxial cable ($l = 5$ m) "lumped model" magnitude of the characteristic impedance per meter.

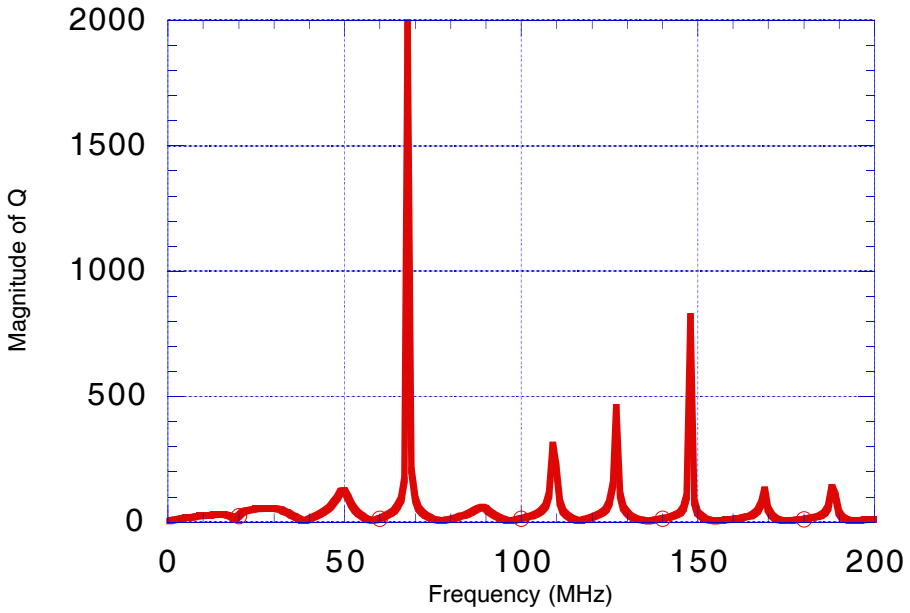

Figure 4.25: Magnitude of Q from 30 kHz to 200 MHz.

account. Looking ahead, Section 4.7 gives further evidence why this model fails.

4.6 Approximations

A more successful method in extracting the L, R, G, and C parameters entails a simple approximation. Looking at the extracted parameters X and Q that were originally derived in Section 4.3 by Equations (4.4) and (4.9), respectively, (see Figures 4.4 and 4.25), it should be noted that the problem of S_{11} going to zero is only prevalent in the magnitude of Q. The plot of the magnitude of X is smooth and has appropriate shape $X = e^{-\alpha d}$. Since the characteristic impedance Z_c is dependent on Q, in order to avoid the points of instability, it becomes necessary to find another approach to extract Z_c.

Since the characteristic impedance of the transmission line is not smooth due to the measurements, as shown in Figure 4.6, the L, R, C, and G parameters have the

problem jumps at the half-wavelength point, when the data extracted characteristic impedance is used in Equations (4.12)-(4.15) shown below for convenience by the group of equations labeled (4.27).

$$\begin{aligned} R &= Re[Z_c \cdot \gamma] \\ L &= \frac{Im[Z_c \cdot \gamma]}{\omega} \\ C &= \frac{Im[\gamma / Z_c]}{\omega} \\ G &= Re[\frac{\gamma}{Z_c}] \end{aligned} \tag{4.27}$$

However, if the characteristic impedance is assumed to be a constant when using Equations (4.27), the L, R, C, and G are readily extracted.

If a line is drawn through the average of the real part of characteristic impedance, as in Figure 4.26, it is easy to see that the characteristic impedance stays relatively constant over the frequency range and that the deviations are caused by the S_{11} jumps which are a cause of the sensitivity of the network analyzer. Assuming that the real part of characteristic impedance does stay constant over the frequency span at 50.2Ω as indicated by Figure 4.26 (Figure 4.6 in Section 4.3 allows for the imaginary part of the characteristic impedance to be ignored) and the γ values are determined using original equation for X in Equations (4.4) and (4.27) allow for the extraction of the sought L, R, C, and G parameters. Figures 4.27, 4.29, 4.31, and 4.35 show the L, R, C, and G parameters over the entire frequency range spanning multiple wavelengths. These figures show that the resistance takes on the square root of frequency form, which is expected as the frequencies increase. Using the inductance and capacitance values extracted the velocity of propagation is extracted $v_p = \sqrt{\frac{L}{C}}$. This approach is also applied toward the Type 2-4 lines and the microstrip line. The results are given in Figures 4.28-4.35.

To summarize this procedure, it is evident that S_{21} and the extracted parameter

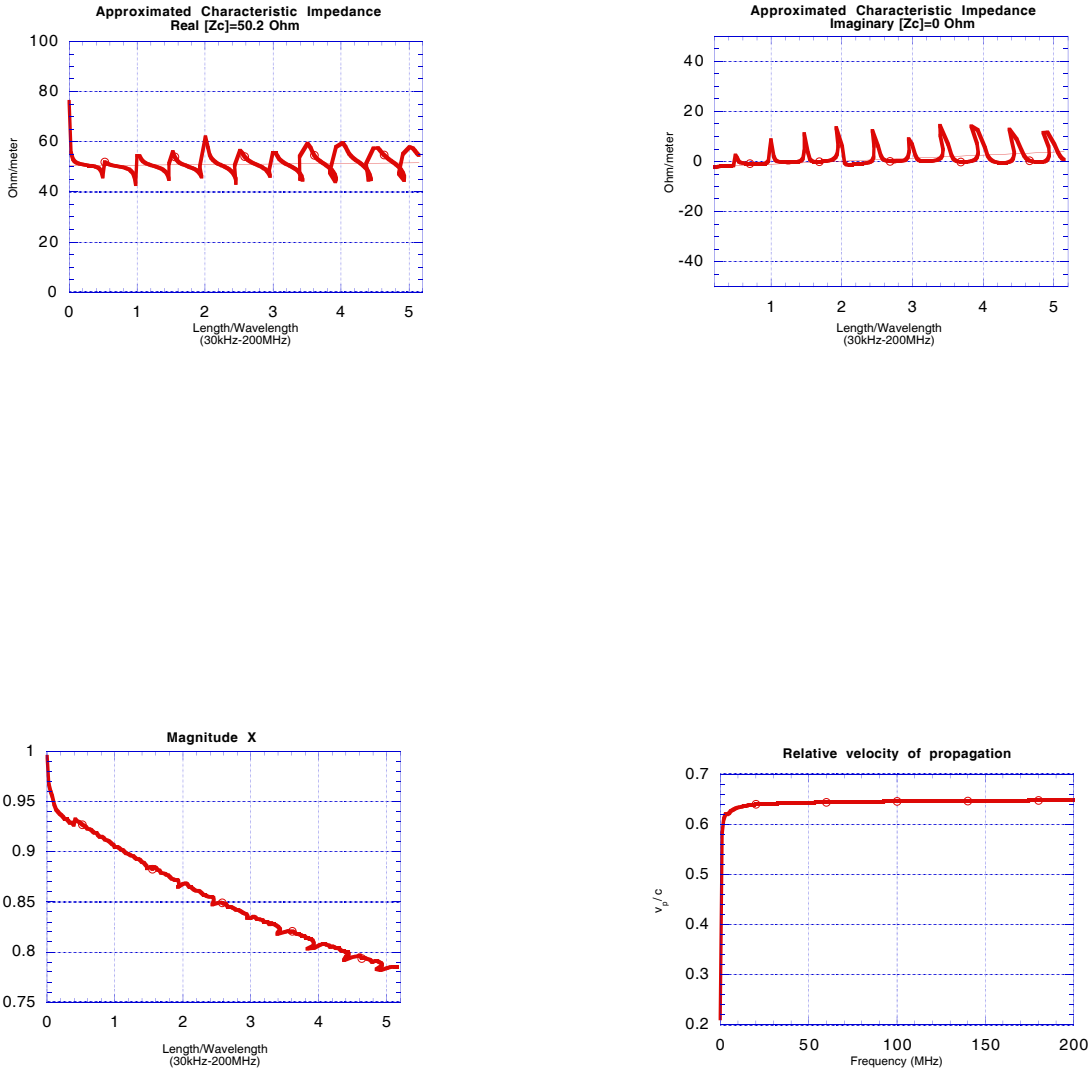

Figure 4.26: Coaxial 50-Ω cable of length $l = 5$ m: Characteristic impedance, magnitude of X, and relative velocity of propagation over multiple wavelengths.

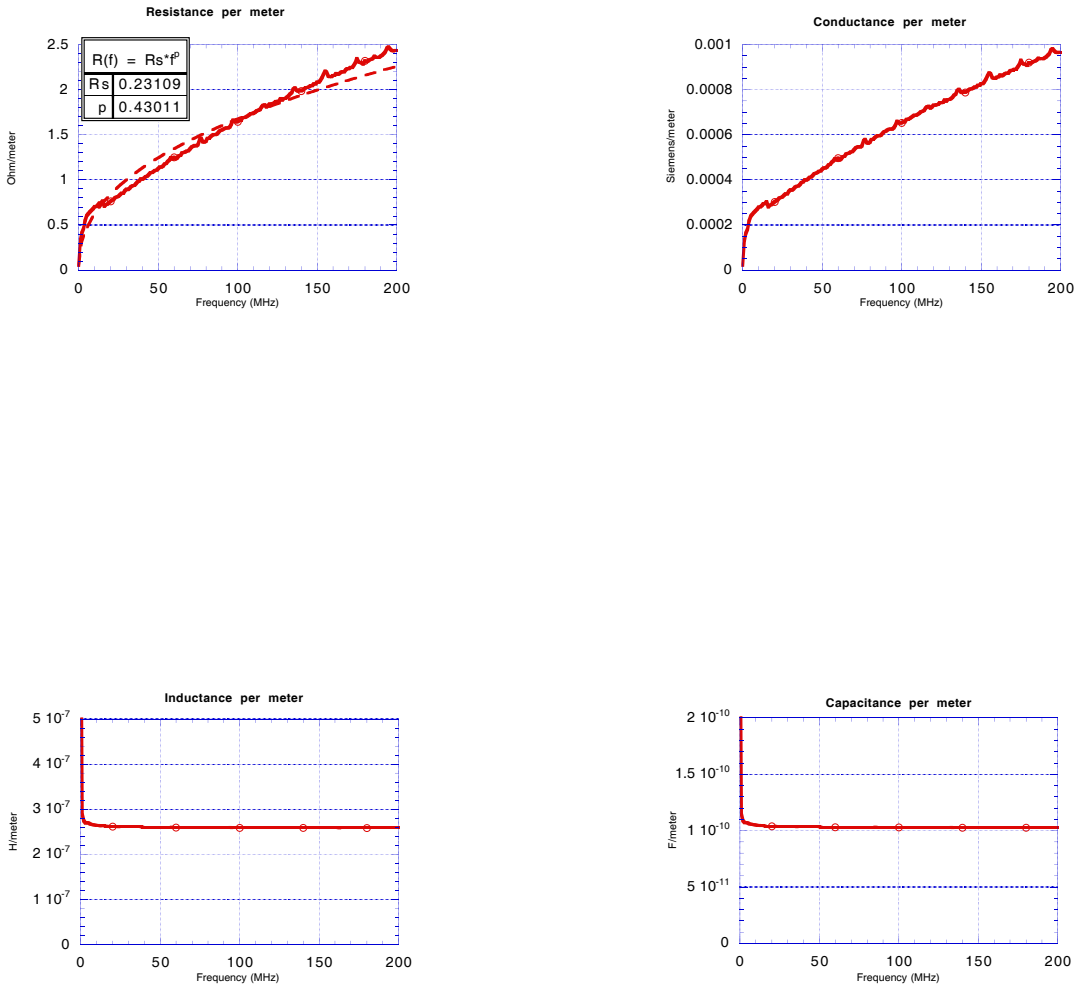

Figure 4.27: Coaxial 50-Ω cable of length $l = 5$ m: L, R, C, and G over multiple wavelengths, using the "wave technique" and characteristic impedance approximation.

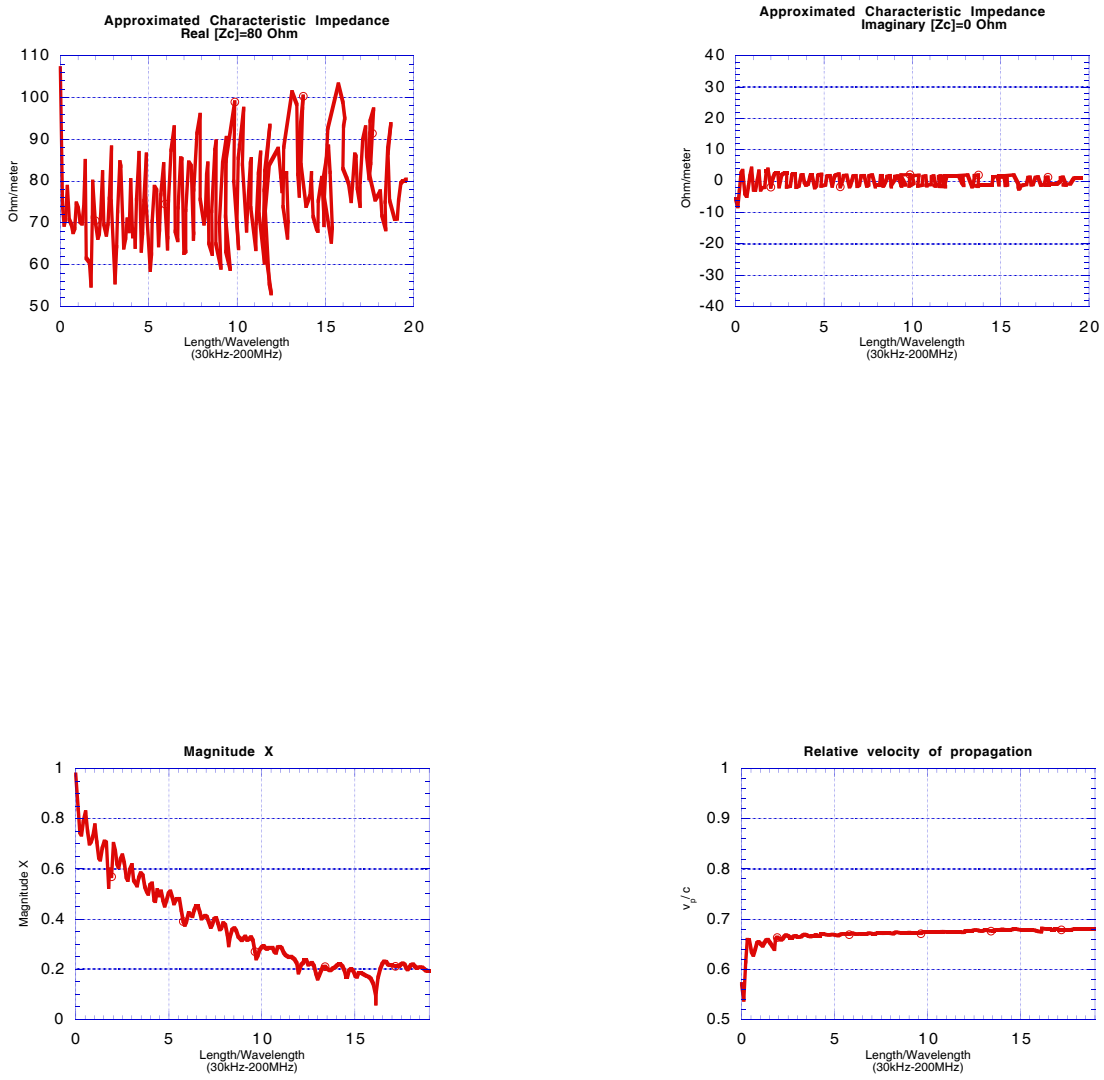

Figure 4.28: Type 2 cable of length $l = 20$ m: Characteristic impedance, magnitude of X, and relative velocity of propagation over multiple wavelengths.

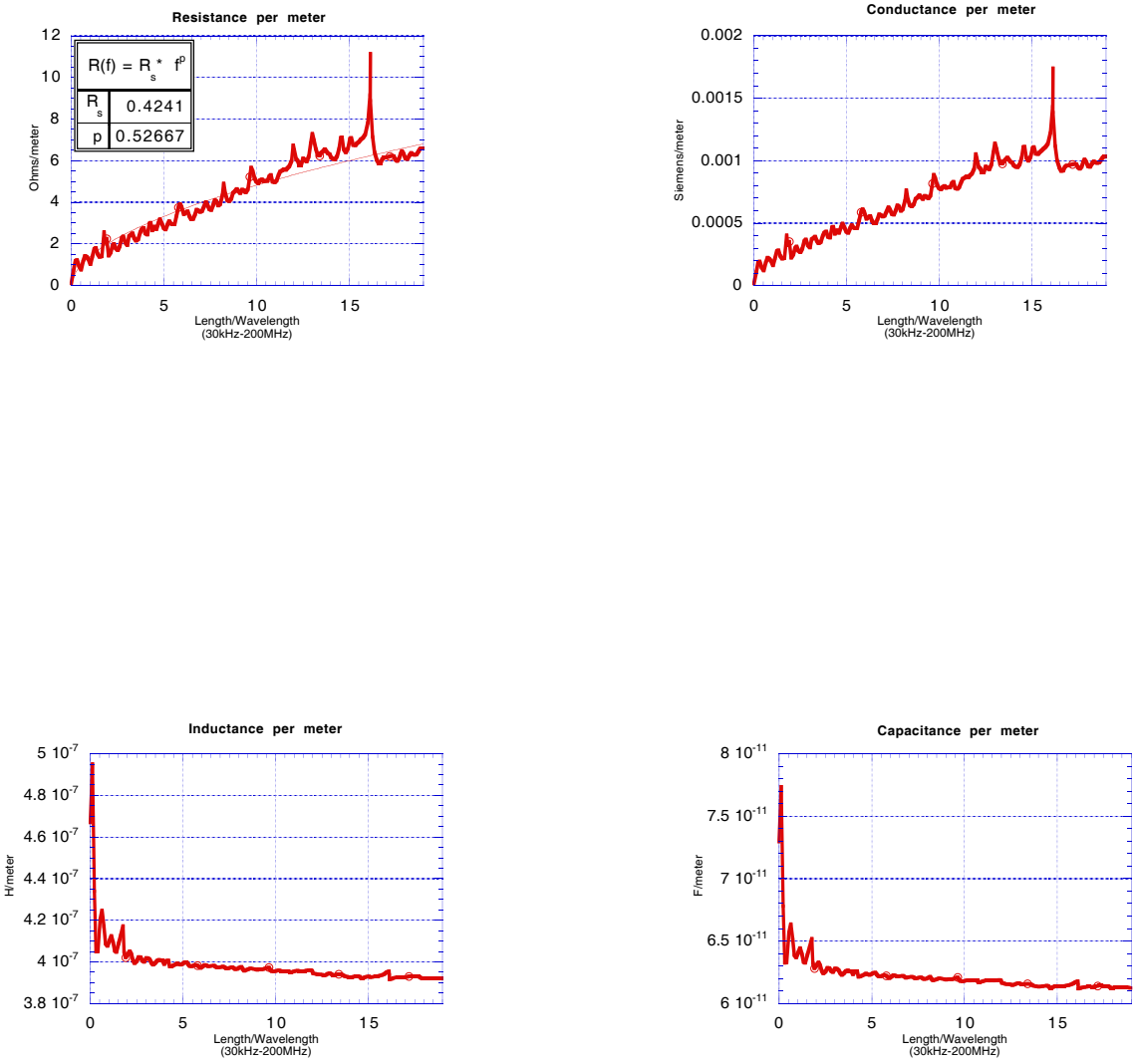

Figure 4.29: Type 2 cable of length $l = 20$ m: L, R, C, and G over multiple wavelengths, using the "wave technique" and characteristic impedance approximation

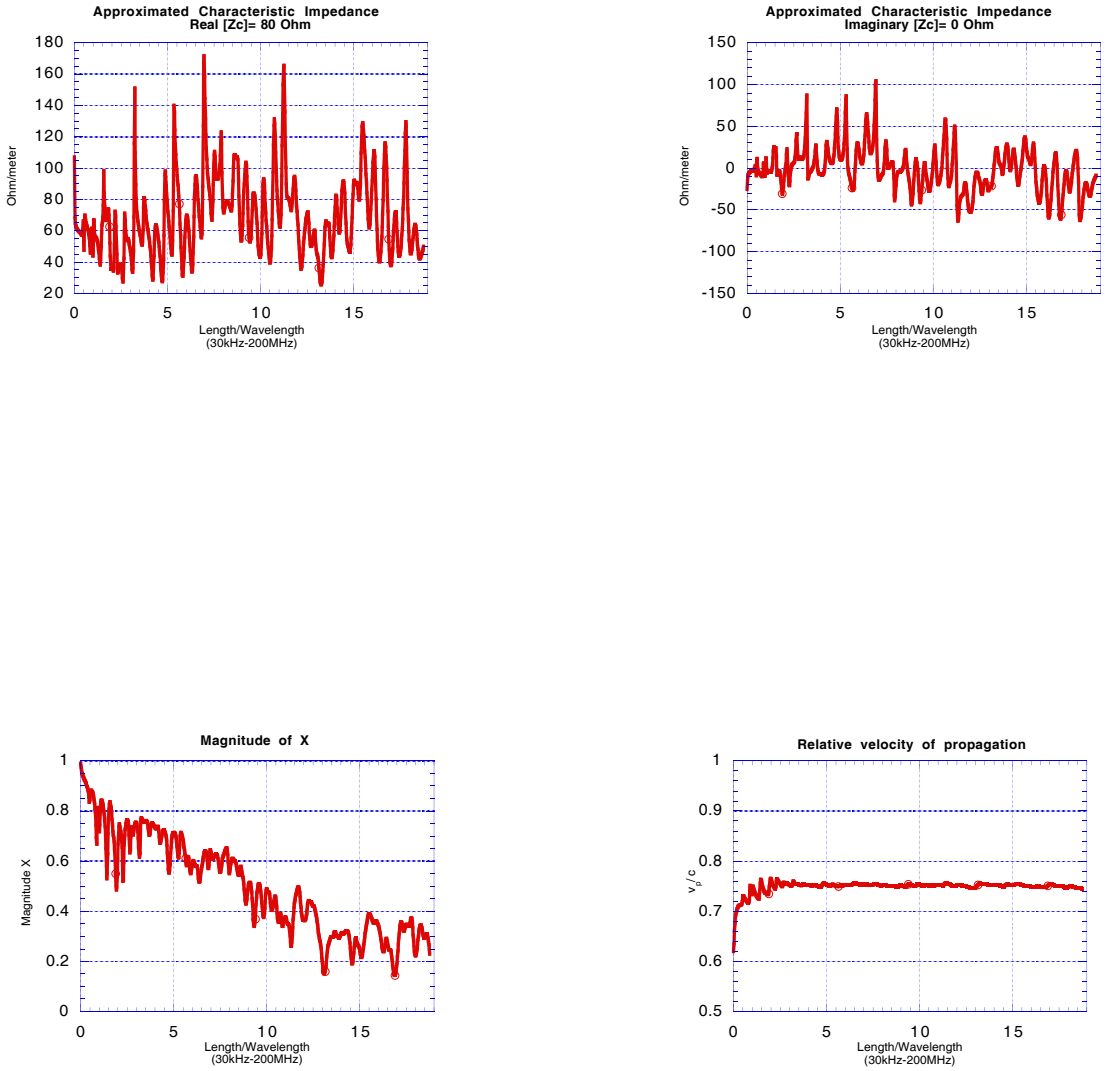

Figure 4.30: Type 3 cable of length $l = 20$ m: Characteristic impedance, magnitude of X, and relative velocity of propagation over multiple wavelengths.

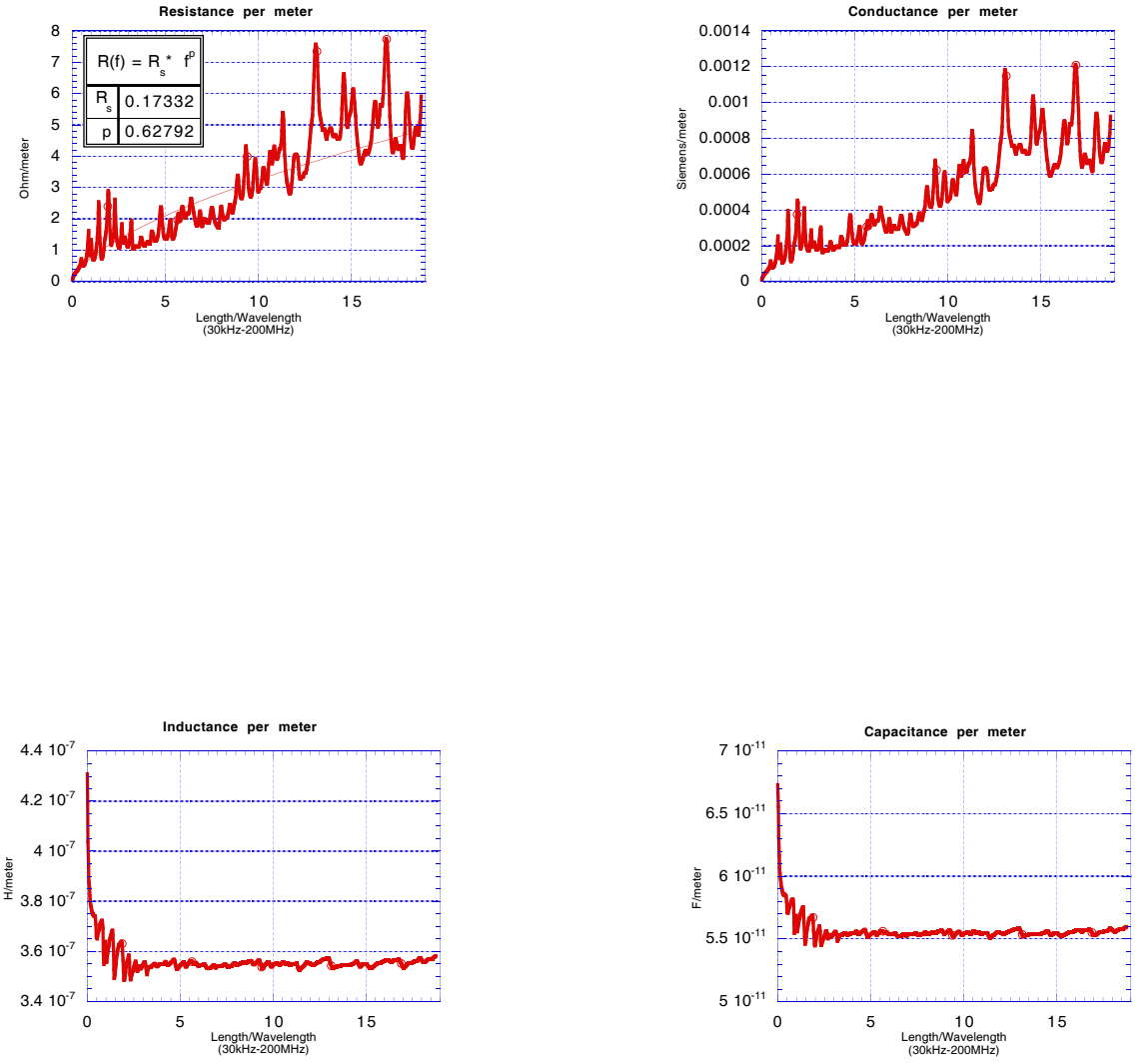

Figure 4.31: Type 3 cable of length $l = 20$ m L, R, C, and G over multiple wavelengths, using the "wave technique" and characteristic impedance approximation.

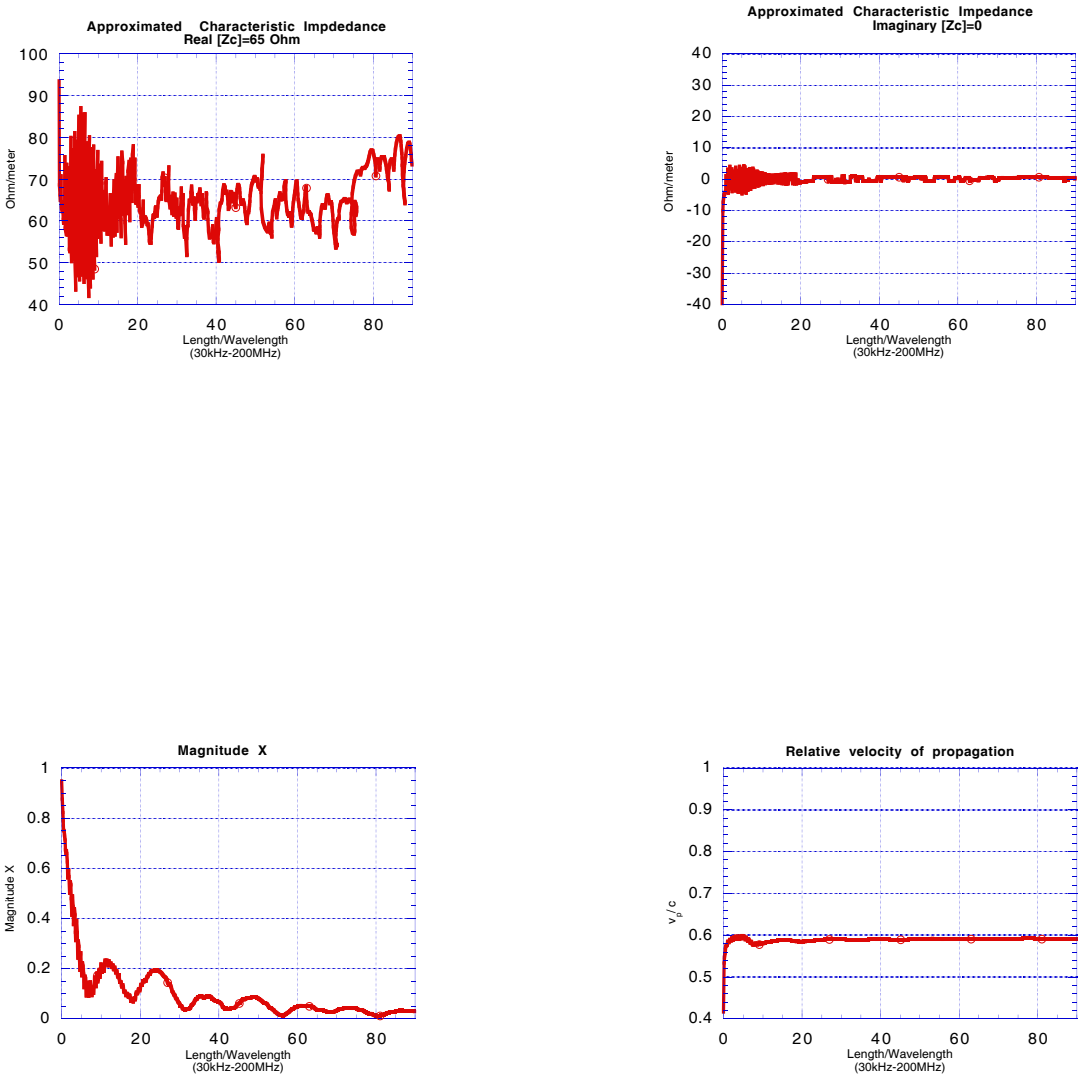

Figure 4.32: Type 4 cable of length $l = 82$ m: Characteristic impedance, magnitude of X, and relative velocity of propagation over multiple wavelengths.

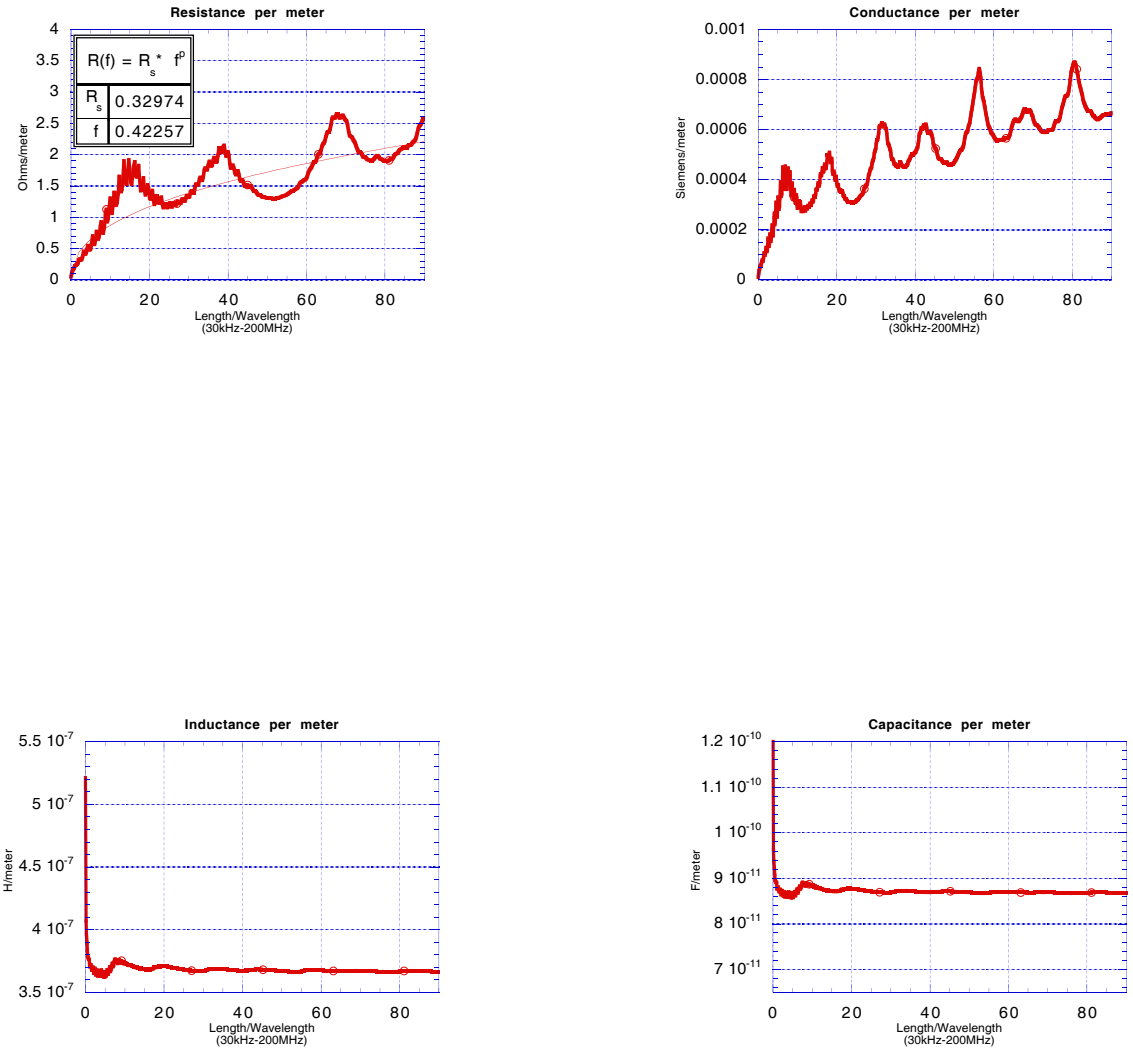

Figure 4.33: Type 4 cable of length $l = 82$ m: L, R, C, and G over multiple wavelengths, using the "wave technique" and characteristic impedance approximation.

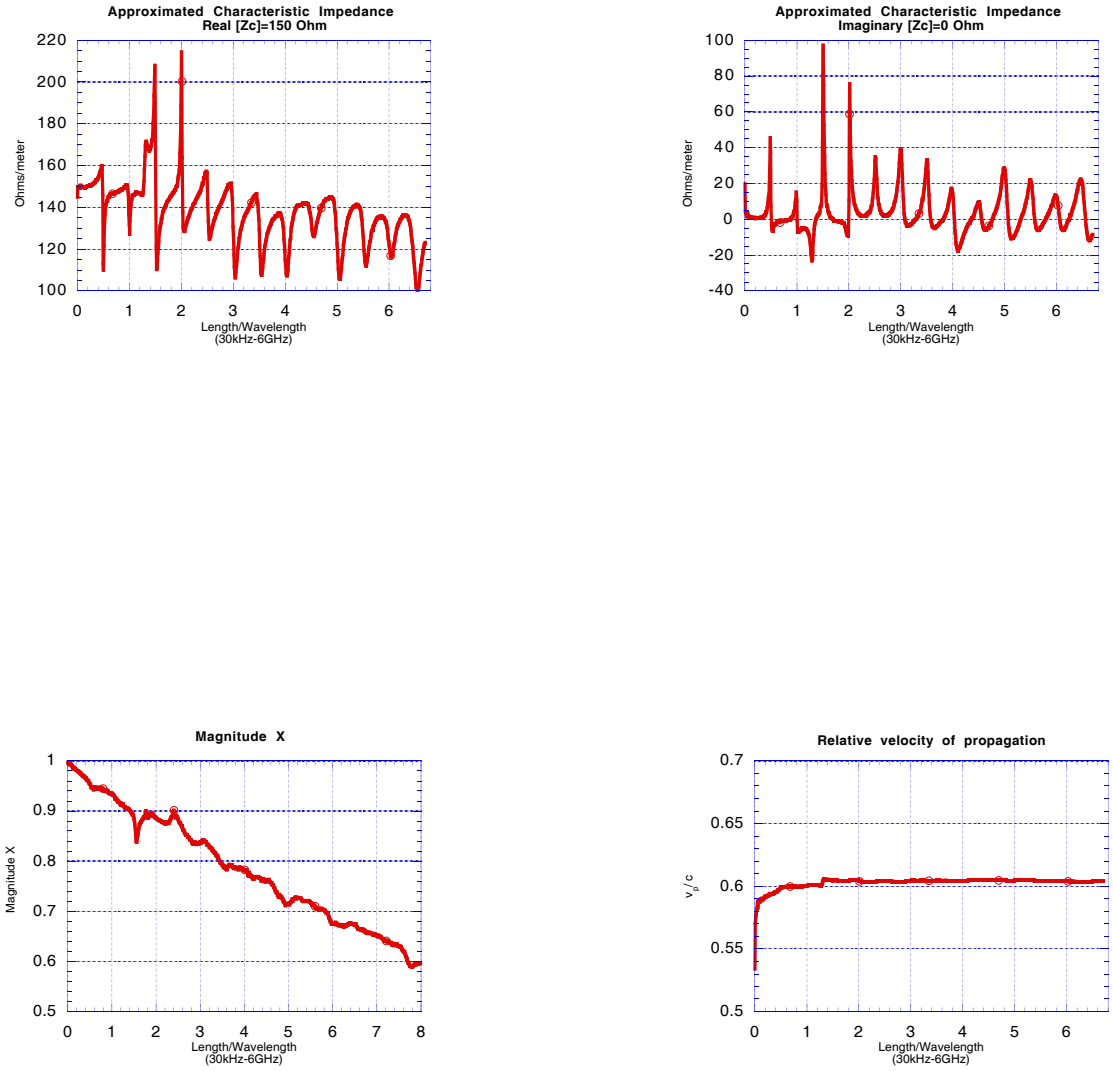

Figure 4.34: Microstrip: Characteristic impedance, magnitude of X, and relative velocity of propagation over multiple wavelengths.

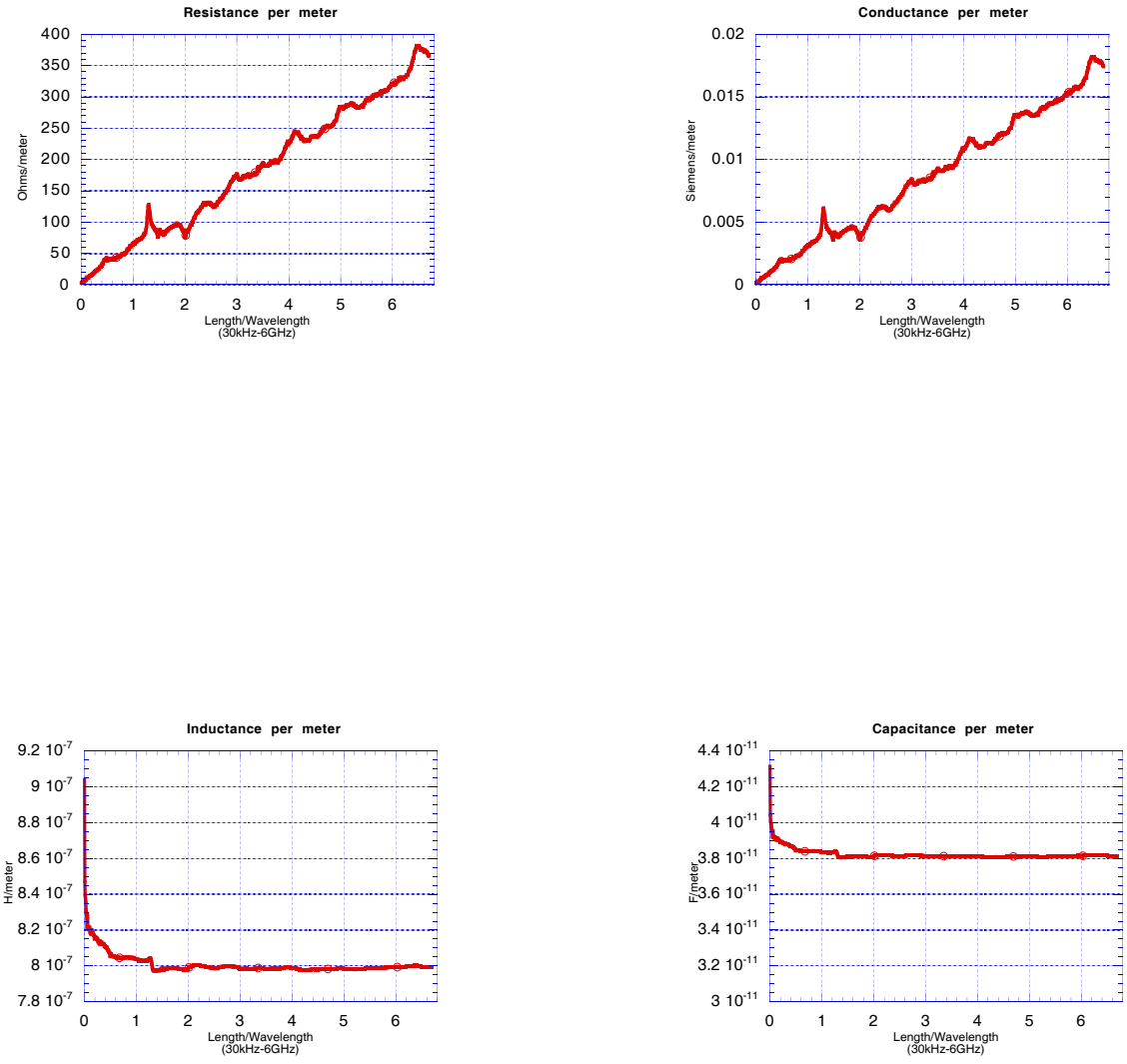

Figure 4.35: Microstrip: L, R, C, and G over multiple wavelengths, using the "wave technique" and characteristic impedance approximation.

$X = e^{\gamma d}$ contain enough of the transmission line propagation information to extract the L, R, C, and G parameters once the characteristic impedance is known. The characteristic impedance is easily calculated form Q, however measurement discontinuities prevent the characteristic impedance Z_c from being constant. By approximating Z_c with the mean of the calculated values for Z_c as done in Figures 4.26, 4.28, 4.30, 4.32, and 4.34, it is possible to extract the L, R, C, and G parameters with γ which is extracted from X.

4.7 Extrapolation

It may be desirable to have a wide frequency range characterization technique using only low frequency scattering parameters. An attempt is made to use the "lumped" model parameters described in Section 4.5, assume the inductance and capacitance stay constant over a large frequency band, and use an equation curve fit to the "lumped" extracted resistance. The problem lies in the fact that in the low frequency range, the resistance does not have the $f^{\frac{1}{2}}$ response as is indicated by Figure 4.36. Although the equation for the curve may be extrapolated into higher frequencies, Figure 4.37 compares this extrapolated resistance with the resistance found using the approximation for the characteristic impedance described in Section 4.6.

Looking at Figure 4.37, it is evident that in the frequency range from 30 kHz to 100 MHz, the "lumped" extrapolated resistance is larger than the "wave" resistance. This may be accounted for by the fact that the lumped model does not take the conductance into account. Though it is usually negligible, it is obviously a factor for this cable. With the lumped model, the loss in the conductance is grouped in with the series resistance loss; thus, an overall larger resistance than the wave model predicts. The wave model takes both the parallel conductance and series resistance

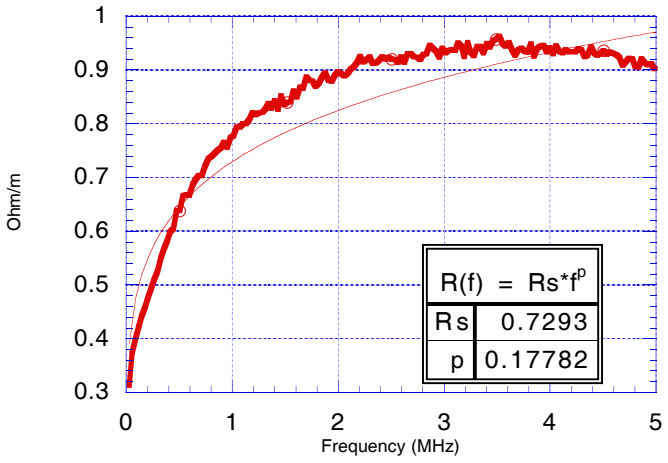

Figure 4.36: Equation fit for low-frequency resistance.

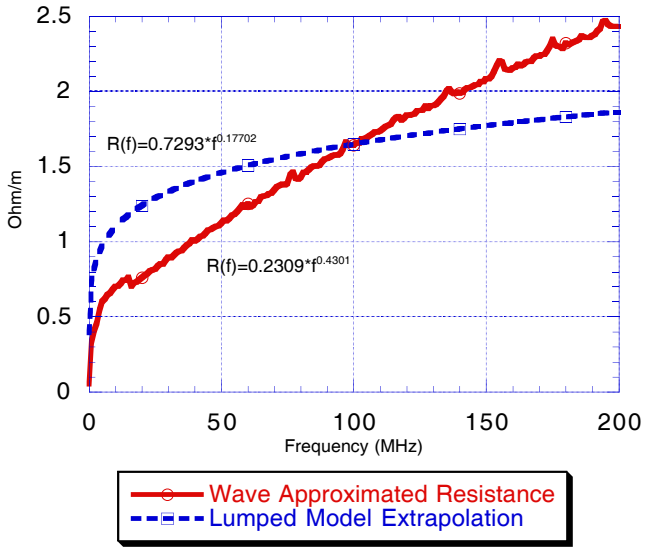

Figure 4.37: This is a comparison of the "wave" approximation approach and the low frequency extrapolation for the resistance of the coaxial line.

into account.

In the frequency range higher than 100 MHz, the lumped model extrapolated curve is lower than the wave extracted curve for the resistance. The low-frequency extrapolation cannot capture the $f^{\frac{1}{2}}$ response the resistance has because it does not span a large enough frequency bandwidth. Over a large bandwidth, the $f^{\frac{1}{2}}$ resistance response becomes evident as Figures 4.27-4.35 indicate; however, this cannot be achieved with the lumped model which is only valid in the low frequency range.

If the low-frequency portion of a $f^{\frac{1}{2}}$ curve is zoomed in on, it does not necessarily look like $f^{\frac{1}{2}}$. In fact, the lower the frequency, the more closely the curve looks like f, a linear response. In conclusion, though an improvement may be made to this lumped model to include the conductance and account for the extra loss, it cannot be used to predict the transmission line response into higher frequencies with much accuracy.

Future work may include using an extrapolation with the parameters extracted with the "wave" technique described in Section 4.3. Since the parameters are easily extracted up to $\lambda/2$, a larger frequency band is available from which to extract the equation curve fit. Again, the "wave" technique already takes the conductance into account, so this parameter does not need to be adjusted.

CHAPTER 5

CONCLUSION

In an attempt to use the "wave" model to characterize transmission lines, it becomes evident that every half-wavelength, S_{11} becomes very small. The sensitivity of the network analyzer does not allow for the exact value of S_{11} to be captured at these frequency points. This discontinuity in the measurement causes "spikes" in the extraction of Γ, the reflection coefficient, and, in turn, the characteristic impedance of the line. This problem is easily avoided in the low frequencies, where the length of the line is less than half a wavelength.

In the low-frequency range, the procedure described in Section 4.3 allows for the extraction of the transmission line parameters: Zc, γ, R, L, G, and C. The lumped model topology described in Section 4.5 fails to account for all the loss due to the parallel conductance, and as a result, the derived series resistance is greater than the more accurate "wave" approach predicts. Furthermore, Section 4.7 shows that the low-frequency data is insufficient to accurately characterize the lines into higher frequencies.

To characterize transmission lines over a wide frequency band covering multiple wavelengths, it becomes necessary to avoid these half-wavelength singularities. Looking back to Section 4.3, it is evident that the division by S_{11} in Equation (4.9) causes the high sensitivity to the small magnitude inaccuracies mathematically. In order to avoid this sensitivity, the measured scattering parameters are numerically converted to ABCD parameters. In this manner, the division by the highly sensitive variable

S_{11} is avoided. It is then feasible to extract the transmission line characteristics directly from the ABCD parameters. This manipulation is an improvement from the extraction described in Section 4.3, as is evident from a comparison of the magnitude of the "spikes" in the extracted resistance from the two techniques shown in Figures 4.7 and 4.15, however, the "spikes" still remain.

The most successful approach for extracting transmission line characteristics is found in Section 4.6. A simple approximation for the characteristic impedance is used in the extraction of all the other characteristic parameters. This approximation avoids the "spikes" that appear at the half-wavelength frequencies. A further improvement in this technique would entail using an equation curve fit for the characteristic impedance. In Section 4.6, the characteristic impedance stays relatively constant; however, it is well known that the characteristic impedance is in fact frequency dependent [8].

REFERENCES

5.1 References

[1] J. Lechleider, "High bit rate digital subscriber lines: A review of HDSL progress," *IEEE J. Sel. Areas Commun.*, vol. 9, pp. 769-784, Aug. 1991.

[2] T. R. Hsing, C. T. Chen, and J. A. Bellisio, "Video communications and services in the copper loop," *IEEE Commun. Mag.*, vol. 1, pp. 62-68, Jan. 1993.

[3] J. J. Werner, "The HDSL environment," *IEEE J. Sel. Areas Commun.*, vol. 9, pp. 785-800, Aug. 1991.

[4] W. Y. Chen, "Broadcast digital subscriber lines," *IEEE J. Sel. Areas Commun.*, pp. 1550-1555, Dec. 1995.

[5] G. Baker, "High-bit-rate digital subscriber lines," *Electron. Commun. Eng. J.*, vol. 4, pp. 279-283, Oct. 1993.

[6] M. Shoji, *High-Speed Digital Ciruits*. Reading, MA: Addison-Wesley, 1996.

[7] H.B. Bakoglu, *Circuits, Interconnections, and Packaging for VLSI*. Reading, MA: Addison-Wesley, 1990.

[8] R. E. Matick, *Transmission Lines for Digial and Communication Networks*. New York: IEEE Press, 1995.

[9] G. Gonzalez, *Microwave Transistor Amplifiers*. Reading, MA: Addison-Wesley, 1996